RESEARCH

Wood Hemicelluloses as Innovative Wall Materials for Spray-Dried Microencapsulation of Berry Juice: Part 1—Effect of Homogenization Techniques on their Feed Solution Properties

Abedalghani Halahlah[1] · Vieno Piironen[1] · Kirsi S. Mikkonen[1,2] · Thao M. Ho[1,2]

Abstract

The use of wood hemicelluloses, including galactoglucomannans (GGM) and glucuronoxylans (GX), in spray-dried microencapsulation of bioactive compounds has not been reported. Our study aims to investigate the benefits of spray-dried GGM and GX powders (sGGM and sGX) along with the effects of homogenization techniques (magnetic stirring, ultrasonication, and a combination of UltraTurrax homogenization and microfluidization) on the physicochemical properties of feed solutions (10–20%, w/w). Feed solutions of bilberry juice with sGGM, sGX, and mixtures of either sGGM or sGX with methylcellulose (MC) or carboxymethylcellulose (CMC) were examined to produce highly stable feed solutions for spray-dried microencapsulation. The effects of ultrasonication amplitudes (30–80%) on the viscosity and particle size distribution of sGGM feed solutions were more profound than observed in their sGX counterparts. Unlike sGX feed solutions, sGGM feed solutions homogenized by ultrasonication and microfluidization formed a gel-like structure. Microfluidization also caused a loss of total anthocyanin content (TAC) of the feed solutions. Magnetic stirring resulted in no gel formation and in the lowest viscosity of the feed solutions; hence, it is an effective method for preparing hemicellulose feed solutions. sGGM and sGX powders have high heat stability with melting temperatures of 170–180 °C. The sGGM + CMC combination was more stable over 1 week of storage than the sGGM and sGX feed solutions. Storing the feed solutions reduced TAC and increased sGGM viscosity. Our results indicated that GGM and GX have high potential for use as wall materials in the spray-dried microencapsulation of bioactive compounds.

Keywords Wood hemicellulose · Microencapsulation · Wall material · Galactoglucomannan · Glucuronoxylan

Introduction

In the spray-dried microencapsulation of bioactive compounds, the selection of a suitable wall material is critical for achieving highest encapsulation efficiency and microcapsule stability (Aghbashlo et al., 2013; Koç et al., 2015). The most common way to select an appropriate wall material or mixture of wall materials is based on their physicochemical properties such as solubility, viscosity, emulsifying properties,

thermal stability, and mechanical properties (Hategekimana et al., 2015; Ramakrishnan et al., 2018). Other important criteria include processing conditions, economic factors, and the intended microcapsule size, in addition to compatibility between the wall and core materials (Hategekimana et al., 2015; Ramakrishnan et al., 2018). Typically, a single wall material will not possess all of the essential properties, and a combination of two or more wall materials with different properties is thus preferred (Favaro-Trindade et al., 2010; Lee et al., 2018). Wall materials can be chosen from a wide range of natural and synthetic polymers, depending on the core material and the desired characteristics of the final product (Belščak-Cvitanović et al., 2015; Estevinho et al., 2013). Most current studies have utilized conventional wall materials (e.g., gum arabics, starches, chitosan, alginate, and maltodextrins), which have major drawbacks in terms of either their emulsifying properties, viability, or sustainability (Belščak-Cvitanović et al., 2015; Ribeiro et al., 2019; Strobel et al., 2020). For

✉ Abedalghani Halahlah
    abedalghani.halahlah@helsinki.fi

[1] Department of Food and Nutrition, University of Helsinki, P.O. Box 66, (Agnes Sjöbergin katu 2), FI-00014 Helsinki, Finland

[2] Helsinki Institute of Sustainability Science (HELSUS), University of Helsinki, P.O. Box 65, FI-00014 Helsinki, Finland

example, maltodextrins do not have strong emulsifying properties because of the presence of hydroxyl groups that promote wettability, presenting a limiting characteristic in the spray-dried microencapsulation process (Agama-Acevedo & Bello-Perez, 2017; Waterhouse et al., 2017). Similarly, native starches (e.g., corn starch) have low emulsifying properties, poor mechanical or barrier properties, and high water sensitivity, thus limiting the retention of hydrophobic bioactive compounds during spray-drying (Coimbra et al., 2020). Although gum arabics have a strong capacity for emulsion stabilization and volatile compound retention (Aniesrani Delfiya et al., 2015), the high costs limit their use. Dairy proteins, the most widely utilized protein-based wall materials, are not derived from sustainable sources due to methane emissions from livestock management (Assadpour & Jafari, 2019; Hindrichsen et al., 2005), and make the produced microcapsules unsuitable for vegans and lactose-intolerant consumers. Wood-based celluloses and their derivatives have been used either as emulsifying agents in the preparation of emulsions for spray-drying or in combination with other wall materials to protect bioactive compounds during spray-drying (Castro-López et al., 2021, Zhang et al., 2017). However, they have high viscosity at high concentrations, which makes spray-dried microencapsulation difficult to accomplish (Halahlah et al., 2022). Therefore, searching for new ecological, cost-effective, and sustainable wall materials is essential for meeting the increasing demand of consumers for "clean" food products/ingredients.

Appropriate homogenization techniques are important in spray-dried microencapsulation, to achieve stable feed solutions, thus ensuring better microencapsulation efficiency and higher stability of the microencapsulated products (Alcântara et al., 2019; Akhtar et al., 2014). Homogenization could incorporate oxygen into the mixed solutions (Kolanowski et al., 2006) and lead to the oxidation of sensitive bioactive compounds (Gambuti et al., 2013). Traditionally, feed solutions are prepared using standard mixing by magnetic stirring. However, ultrasonication homogenization was found to produce more stable feed solutions with smaller-sized dispersed droplets in them, and this contributed to a stability increase in the produced microcapsule powders and microencapsulation efficiency (Alcântara et al., 2019). Similar effects of ultrasonication on the stability of feed solution and the spray-dried microencapsulation efficiency of coconut milk fat were also reported (Du Le & Le, 2015). However, high-powered ultrasonication of feed solutions over a long time period resulted in the formation of large-sized aggregates, leading to a drop in microencapsulation efficiency and yield. The use of high-speed homogenization (e.g., UltraTurrax) and/or its combination with high-pressure homogenization for preparing feed solutions of green coffee oil was also investigated (Silva et al., 2014). Compared with UltraTurrax alone, the combined use of high-pressure homogenization further decreased droplet size and viscosity, and consequently increased microencapsulation efficiency. Nonetheless, the homogenization speed of UltraTurrax

reportedly had a great effect on the phenolic content of propolis powder, causing lower recovery of phenolic compounds at a higher homogenization speed (Baysan et al., 2019). Investigating various approaches for feed solution preparation is therefore very important for maximizing microencapsulation efficiency and yield and for obtaining microcapsule powders with desirable properties.

Hemicelluloses constitute 20–30% of wood dry mass (Kirjoranta et al., 2020), but they are currently treated as low-value by-products of the forest industry. During cellulose refining, hemicelluloses typically end up in waste pulping liquor and/or are burned for energy (Valoppi et al., 2019a). Hemicelluloses, including galactoglucomannans (GGM) from spruce wood and glucuronoxylans (GX) from birch wood, have been successfully extracted using a highly safe and environmentally friendly method known as pressurized hot water extraction (PHWE) (Kilpeläinen et al., 2014). This enables the extracted hemicelluloses to be used in many food products (Kirjoranta et al., 2020; Valoppi et al., 2019b). The backbone of GGM is made of $(1 \rightarrow 4)$-linked β-D-mannopyranosyl (Man$p$) units and $(1 \rightarrow 4)$-linked β-D-glucopyranosyl units, and some α-galactopyranosyl units are $(1 \rightarrow 6)$-linked to the backbone as single-unit side groups (Lahtinen et al., 2019). The GX backbone is made of $(1 \rightarrow 4)$-linked β-D-xylopyranosyl (Xyl$p$) units, to which α-4-O-methylglucuronic substituents are $(1 \rightarrow 2)$-linked (Lahtinen et al., 2019; Teleman et al., 2002). The O-acetyl groups are present in both GGM and GX at the C-2 and/or C-3 positions of the Man$p$ and Xyl$p$ units. Acetylation levels have been found to be around 15–20% for GGM and 25% for GX (Du et al., 2013). In aqueous solution, GX has less insoluble fractions than GGM (Lahtinen et al., 2019). The PHWE wood hemicelluloses are intermediate in molar mass with 10,000 g/mol and 6500 g/mol reported for GGM and GX, respectively (Mikkonen et al., 2016). As a result, GGM and GX have low viscosity in aqueous solutions (Kirjoranta et al., 2020), enabling their spray-drying with ease. GGM and GX have been demonstrated as excellent stabilizers in dispersed systems such as oil-in-water emulsions (Bhattarai et al., 2019; Valoppi et al., 2019a). Their ability to protect emulsions against physical breakdown and lipid oxidation was found to be better than that of gum arabic and corn fiber gum (Bhattarai et al., 2019; Lehtonen et al., 2018). GGM and GX also contain lignin-derived phenolic residues that are assumed to contribute to emulsion stabilization by introducing an amphiphilic character to GGM and GX (Xu et al., 2009). All these reported properties of GGM and GX, along with their abundant, sustainable, and low-cost sources, indicated that they are possibly excellent wall materials for the spray-dried microencapsulation of bioactive compounds. However, such application of GGM and GX, especially for spray-dried microencapsulation of high anthocyanin and phenolic materials, such as bilberry, has not been investigated.

Bilberries were chosen for this study as they are the most important commercially traded berry in the Nordic region (Ovaskainen et al., 2008). They have a high content of phenolic compounds (e.g., anthocyanins, flavonols, proanthocyanidins, and phenolic acids), vitamins (A, C, and E), and dietary fibers. The sustainability (grow abundantly in Nordic forests) and exceptional nutritional value of bilberries makes them a unique material and has led to a great increase in their global demand as functional and natural products (Esfanjani et al., 2018).

In this study, we evaluated the applicability of wood hemicelluloses as wall materials for producing spray-dried microcapsules of bilberry juice in comparison to the most widely foraged commercial wood celluloses including methylcelluloses (MC), carboxymethylcelluloses (CMC), and cellulose nanocrystals (CNC). The investigated hemicelluloses include (1) spray-dried GGM and GX that were obtained by PHWE followed by spray-drying, (2) ethanol-precipitated GGM and GX, and (3) carboxymethylated GGM and GX. Ethanol precipitation removes part of the lignins while carboxymethylation enhances the anionic character of hemicelluloses, both of which are demonstrated to improve the water solubility of hemicelluloses (Gabriel et al., 2020). The study focuses on investigating the thermal properties of hemicelluloses and the effects of different homogenization techniques (magnetic stirring, ultrasonication, and a combination of high-speed homogenization of UltraTurrax and microfluidization) on the physiochemical properties of feed solutions of bilberry juice to obtain a stable feed solution. The evaluation criteria for feed solutions include total anthocyanin content (TAC), viscosity, ζ-potential, surface charge density, particle size distribution, and physical sedimentation kinetics. The study also provides further insights on the effect of ultrasonication (amplitude) and mirofluidization (number of passes) on the physiochemical properties of feed solutions.

Materials and Methods

Materials and Reagents

Extracts of GX and GGM were recovered from wood saw dust by semi-pilot-scale PHWE, as described by Kilpeläinen et al. (2014) and provided by the Natural Resources Institute Finland (Luke). The extracts were then spray-dried (sGX and sGGM) and further treated with either ethanol precipitation (eGGM and eGX) or carboxymethylation (CMGGM and CMGX). The spray-drying process was carried out using a pilot-scale spray-dryer (Mobile-minor; Niro Atomizer Co., Ltd., Copenhagen, Denmark) at an inlet temperature of 180 °C and an outlet temperature of 70 °C (Valoppi et al., 2019a). The ethanol-precipitated hemicelluloses were prepared according to Song et al. (2013) by adding the aqueous

solutions of GGM or GX (30% w/w) to ethanol (1:8 v/v) and left to precipitate overnight. The supernatants were then decanted, the precipitates were filtered and washed with ethanol, and finally dried. Carboxymethylated hemicelluloses were prepared according to the method described by Xu et al. (2011). Aqueous sodium hydroxide was gently added to the slurry of GGM or GX solutions while continually stirring, then small portions of solid sodium monochloroacetate were introduced to the mixture (after 15 min). The reaction mixture was maintained at 50 °C for 3 h. The crude sediment of carboxymethylated hemicelluloses was purified by dissolving it in a small water amount and then gently added to methanol to achieve a final volume ratio of 1:9 under stirring. The carboxymethylated hemicelluloses was then recovered by filtration. Commercial bilberry juice was bought from a local supermarket (Marjex, Helsinki, Finland). The juice contained 10.2% carbohydrate mainly composed of sugars, 0.8% proteins, and 0.6% fat. The soluble solid content of bilberry juice measured by a digital refractometer (PAL-1; Atago Co. Ltd., WA, USA) was about 10%.

MC (Methocel A15 Premium) and Na-CMC (Texturecel CRT 30 PA) were kindly provided by Coloron Company Ltd. (Dartford, UK) and DuPont Company (Delaware, USA), respectively. The anionic cellulose nanocrystal (aCNC) and desulfated non-ionic cellulose nanocrystal (dCNC) were purchased from Cellulose Lab (Fredericton, Canada). Potassium chloride, sodium hydroxide, and sodium acetate were bought from Merck (Massachusetts, USA). Ethanol (≥ 99.5%) was purchased from Altia (Helsinki, Finland). Methanol was obtained from Sigma-Aldrich (Helsinki, Finland). Polydimethyl-diallyl-ammonium chloride (polyDADMAC) was purchased from BTG Instruments AB (Saffle, Sweden). Milli-Q water was used as a solvent for all experiments.

Screening Celluloses and Hemicelluloses for Applicability as Wall Materials

We conducted an initial screening and comparison between the aqueous solutions (20% w/w) of eGGM, eGX, sGGM, sGX, CMGX, and CMGGM prepared by magnetic stirring (600 rpm for 30 min). The evaluation was based on solubility, viscosity, and sedimentation kinetic behavior (data not shown). The results indicated the similarity of these properties among the investigated samples. However, sGGM and sGX production is more environmentally friendly and lower in production costs than eGGM, eGX, CMGX, and CMGGM production. The preparation of eGGM and eGX generated a large amount of ethanol waste and was of relatively low yield (~60%). Furthermore, ethanol treatment removes a large portion of the phenolic compounds that exist naturally in GGM and GX, and contributes greatly to enhancing their emulsifying properties (Kirjoranta et al., 2020). Similarly, a yield of only 50% was obtained in the production of CMGGM and

CMGX, and toxic solvents (e.g., sodium hydroxide) were involved in the process. Aqueous solutions of either aCNC or dCNC have very high viscosity, even at low concentrations (e.g., 15–20 mPa.s for 1% w/w solution), which makes spray-drying very challenging. We therefore selected sGGM, sGX, MC, and CMC for further investigation.

Thermal Properties of Hemicelluloses and Celluloses

The thermal properties of selected hemicellulose (sGGM and sGX) and cellulose (MC and CMC) powders were determined using a differential scanning calorimeter (DSC823e; Mettler-Toledo AG, Greifensee, Switzerland). An 8–10-mg sample was weighed in a 40-µL aluminum pan, sealed hermetically, and scanned at a heating rate of 5 °C/min from 25 to 200 °C. The measuring cell was flushed with flowing nitrogen gas to prevent water condensation. Determinations of baseline changes in the heat flow signal, associated with glass transition temperature (T_g), were characterized by the onset and peak temperatures. The onset temperature was taken as T_g. The sharp endothermic peaks were identified as melting temperature (T_m). The experiments were performed in triplicate, and values are reported with water activity (a_w).

Preparation of Feed Solutions Using Homogenization Techniques

Preparation of Wall Material Solutions

We did not dissolve wall materials directly into the bilberry juice to avoid introducing oxygen into the solutions while stirring, which could lead to oxidation of the anthocyanins present in the juice. Also, using heating when preparing the MC and CMC solutions may cause the degradation of bioactive compounds if bilberry juice is used as a solvent to dissolve MC and CMC. The concentration of hemicellulose solutions at 10% (w/w) was chosen based on

preliminary trials, which indicated that the visual precipitation of hemicelluloses was noticeable at higher concentrations (e.g., ~ 20% w/w). The CMC solution (7% w/w) was dissolved in warm water at 45–50 °C and left to be stirred overnight at room temperature until complete dissociation. The MC solution (6% w/w) was dissolved using the hot–cold water method (Nasatto et al., 2015). Briefly, approximately 1/3 of the required water volume was heated to at least 85 °C, then the MC powder was added to the pre-heated water with agitation until the powder was thoroughly wetted and evenly dispersed. The remaining water (2/3) was then added as cold water (~ 5 °C) to decrease the dispersion temperature. To achieve complete solubilization, the dispersed solution was kept under agitation (300 rpm) for 20–40 min. The selected concentrations of CMC and MC solutions were due to their higher viscosity at higher concentrations. In addition, the MC solutions formed insoluble clumps at higher concentrations.

Preparation of Feed Solutions Consisting of Wall Material and Bilberry Juice

Feed solutions of either sGGM, sGX, MC, CMC (single wall material), or sGGM + MC, sGGM + CMC, sGX + MC, sGX + CMC (wall material mixture) with bilberry juice were prepared with solid ratios, as indicated in Table 1. Previous investigations have demonstrated that certain hemicelluloses have high affinity toward celluloses and that the hemicellulose side groups play a crucial role in the degree of affinity (Lucenius et al., 2019; Naidjonoka et al., 2020). Therefore, the presence of celluloses in the wall material system is expected to improve the protection of bioactive compounds during the spray-dried microencapsulation of hemicelluloses. Mixing two or more wall materials could improve the encapsulation efficiency and product yield as a result of a higher wall material-to-core material ratio (Mahdi et al., 2020; Nunes et al., 2018; Sansone et al., 2011). However, higher wall material-to-core material ratio could have a

Table 1 Solid ratios between wall materials and bilberry juice in feed solutions

Sample codes	Wall materials	Wall material-to-juice solid ratio (w/w)
sGGM	Spray-dried galactoglucomannan/bilberry juice	1:1
sGX	Spray-dried glucuronoxylan/bilberry juice	1:1
MC	Methylcellulose/bilberry juice	0.6:1
CMC	Carboxymethylcellulose/bilberry juice	0.7:1
sGX + MC	Spray-dried glucuronoxylan/methylcellulose/bilberry juice	1:0.6:1
sGX + CMC	Spray-dried glucuronoxylan/carboxymethylcellulose/bilberry juice	1:0.7:1
sGGM + MC	Spray-dried galactoglucomannan/methylcellulose/bilberry juice	1:0.6:1
sGGM + CMC	Spray-dried galactoglucomannan/carboxymethylcellulose/bilberry juice	1:0.7:1

For wall material mixtures (e.g., sGGM + MC, sGGM + CMC, sGX + MC, and sGX + CMC), the solid ratios between hemicelluloses (e.g., sGGM and sGX) and celluloses (MC and CMC) were 1:0.6 and 1:0.7, respectively

negative impact on the encapsulation efficiency and product yield which was explained due to the increase in the viscosity of feed solutions as wall material concentration increased (Di Battista et al., 2015, Negrão-Murakami et al., 2017; Oliveira et al., 2018; Castro-López et al., 2021). Feed solutions were prepared in triplicate and used for further experiments.

Homogenization Techniques

Standard Mixing with a Magnetic Stirrer

Agitation was performed at room temperature (22 °C) in closed Duran glass bottles (100 mL) to avoid introducing oxygen that may induce the degradation of phenolic compounds and anthocyanins of bilberry juice (Oliveira et al., 2015). All the experiments were performed in triplicate with a stirring speed of 600 rpm for 30 min (Heidolph Instruments GmbH, Schwabach, Germany).

Ultrasonication

Ultrasonic irradiation was applied utilizing a digital sonifier (Branson 450 W, Branson, Danbury, USA). The instrument was operated at a fixed frequency of 20 kHz and equipped with a cylindrical titanium alloy probe (12.70 mm in diameter), which was immersed to the same depth inside the feed solution vials. The experiments were conducted at three sonication amplitude levels (30%, 55%, and 80%) for 5 min. The samples were placed in an ice bath to keep the temperature stable during ultrasonication. All the experiments were performed in triplicate.

A Combination of High-Speed Mixing and Microfluidization

The feed solutions were premixed using an UltraTurrax (T-18 basic; IKA, Staufen, Germany) equipped with a disperser-type stirrer at 11,000 rpm for 2 min. The premixed feed solutions were then subjected to a high-pressure homogenizer (Microfluidizer 110Y; Microfluidics, Westwood, MA, USA) at 800 bar for different numbers of passes (1, 3, and 5). The temperature was kept low by circulating cold water during the process to avoid any temperature interference. To simplify the presentation, the term "microfluidization" is hereafter used to refer to this homogenization technique. All the experiments were performed in triplicate.

Analytical Methods for Properties of Feed Solutions

Total Anthocyanin Content

The total anthocyanin content (TAC) of bilberry juice and feed solutions were estimated spectrophotometrically using the pH differential method (Giusti and Wrolstad, 2001). The solution was diluted with two buffer solutions of pH 1.0 (potassium chloride, 0.025 M) and pH 4.5 (sodium acetate, 0.4 M). The absorbance of each dilution was measured at 510 nm (A_{510}) and 700 nm (A_{700}) against a distilled water control using UV–Vis spectrophotometer (UV-1800; Shimadzu, Kyoto, Japan). TAC was obtained from the following equation:

$$TAC = \frac{A \times MW \times DF \times 1000}{\varepsilon \times l}, \tag{1}$$

where $A = (A_{510} - A_{700})\, pH_{1.0} - (A_{510} - A_{700})\, pH_{4.5}$, MW is the molecular weight (where MW of cyanidin-3-glucoside = 449.2 g/mol), DF is the dilution factor, ε is the molar absorptivity (ε of cyanidin-3-glucoside = 26,900), and l = path length (1 cm). TAC was expressed as milligrams of cyanidin-3-glucoside equivalents per liter of juice. Cyanidin 3-O-glucoside is the most abundant anthocyanin in bilberry fruits (Ponder et al., 2021).

Surface Charge Density

The charge density of feed solutions was determined by an aqueous streaming current with a particle charge detector (PCD-05; BTG Mütek, Hershing, Germany). Each feed solution was diluted 20 times, except for the CMC feed solution, which was diluted 100 times. The pH of all the feed solutions was in the range of 3.7–3.9. The samples were then titrated with 0.001 N polyDADMAC, until the streaming potential reached its isoelectric point (charge = 0 mV). Based on the amount of polyDADMAC added to neutralize the charge of each polymer, the charge density was calculated according to the following equation:

$$q = V \times \frac{C}{m}, \tag{2}$$

where V is the consumed titrant volume (L), c is titrant concentration (eq/L), m is solids of sample or its active substance (g), and q is the specific charge density (eq/g).

ζ-Potential

The ζ-potential of feed solutions was determined by the dynamic light scattering technique using a Zetasizer Nano ZS (Model Zen 3600; Malvern Instruments Ltd., Worcestershire, UK) equipped with a laser (4 mW, 632.8 nm) and backscatter detection at 173° to eliminate the effect of multiple scattering. Folded capillary cells were used at 25 °C. At least three measurements, with 15 − 30 runs per measurement, were performed for each sample. All samples were diluted 1000 times in mQ water.

Viscosity Measurement

The viscosity measurements of the feed solutions were performed with a rotational Haake rheometer (RheoStress 600; Thermo Fisher Scientific, Waltham, MA, USA). The cone-and-plate geometry was used, with a diameter of 60 mm and a 2° cone angle. The sample compartment was controlled at a temperature of 20 °C using a water bath/circulator (Haake DC-30). The measurements were carried out with a gap distance of 0.2 mm between cone and plate at a shear rate ranging from 3 to 1500 1/s. The viscosity values were reported at a shear rate of 100 1/s. All the experiments were performed in triplicate.

Particle Size Distribution

Particle size distributions in the feed solutions were determined by the static light scattering technique using a particle size analyzer (Mastersizer Hydro 3000; Malvern Instruments). The refractive index used was 1.53 for hemicelluloses and 1.33 for water. The feed solutions were diluted or added directly into the dispersion accessory and left to agitate for approximately 5 min to avoid multiple scattering effects. The rotor speed during measurement was 2400 rpm. All the experiments were performed in triplicate.

Physical Stability

The physical stability of feed solutions was evaluated using a Turbiscan Lab Expert analyzer (Formulaction; Smart Scientific Analysis, Toulouse, France). In this technique, a detection head with a pulsed near-infrared light source ($\lambda = 850$ nm) and two synchronous detectors were used to measure the light transmission and backscattering of the samples. The detection head moved up and down inside a cylindrical cell to acquire data from transmission and backscattering (one scan takes 20 s). From the prepared feed solutions, 20 mL was poured into a semi-flat-bottom-shaped glass vial and kept undisturbed at room temperature. The vials were intermittently scanned over a period of 1 week. The Turbiscan stability index (TSI), obtained from Turbisoft (version 1.2; Formulaction), was used as a basis for evaluating the physical stability of the feed solutions. An increase in TSI values over time indicated a reduction in feed solution stability. At least three replicates of each sample were prepared and measured.

Feed Solution Stability during Storage

Actual spray-dried microencapsulation operations often require a considerable time to prepare and complete the spray-drying procedures, during which feed solutions must be stable and bioactive compounds are not lost. In this section, we investigated the changes in the properties of selected feed solutions over a week of storage. The sGGM, sGX, and sGGM + CMC feed solutions prepared by magnetic stirring were chosen for this study because they have shown the highest potential as wall materials for spray-dried microencapsulation among the investigated samples and homogenization conditions. Further details are explained in "Feed Solution Stabilities" section.

The feed solutions of sGGM, sGX, and sGGM + CMC with compositions and solid concentrations illustrated in "Preparation of Feed Solutions Consisting of Wall Material and Bilberry Juice" section were homogenized by magnetic stirring, as described in "Standard Mixing with a Magnetic Stirrer" section. The samples were kept in 50-mL falcon tubes and stored at room temperature (22 °C) in darkness. After predetermined interval storage time, the samples were taken for analyses of viscosity, TAC, ζ-potential, particle size, and TSI by following the procedures described in "Analytical Methods for Properties of Feed Solutions" section. Feed solutions were prepared in triplicate.

Statistical Analysis

One-way ANOVA followed by post hoc Tukey's test was performed to differentiate the mean values of the homogenization techniques. The data were tested for normal distribution by analyzing the residuals. The analysis was performed with JMP Pro 13 (SAS, Cary, NC, USA) at a confidence level of 95%.

Results and Discussion

Thermal Analysis

A differential scanning calorimeter (DSC) is important for determining the thermal stability of wall materials for spray-dried microencapsulation, as indicated in a previous study (Iturri et al., 2021). The authors concluded that DSC analysis is essential for setting spray-drying temperatures and for evaluating the applicability and concentration of wall materials to obtain spherical microparticles. The spray-dried microencapsulation of bioactive compound-rich materials is usually carried out at an inlet air temperature below 200 °C to minimize the loss of bioactive compounds (Fazaeli et al., 2012; Ferrari et al., 2012; Nogueira et al., 2020). Thereby, we evaluated the thermal stability of the sGGM, sGX, MC, and CMC powders under DSC scanning up to 200 °C, and the results are presented in Fig. 1a. The DSC curve of sGX ($a_w = 0.27$) revealed a major transition at 56–64 °C while the sGGM curve ($a_w = 0.33$) exhibited two major transitions at approximately 85–91 °C and 122–135 °C. These transitions are suggested to be linked to the T_g of lignin presenting in hemicelluloses (Olsson &

Salmén, 1997; Stelte et al., 2011). Besides the difference in molecular weight between sGGM and sGX, the differences in acetylation degree, the side groups in their structure, and the residual sugars could also explain the considerably higher T_g of sGGM compared with sGX. According to Gröndahl et al. (2003), the T_g of sGX extracted from aspen wood has varied depending on the degree of acetylation and on the extraction methods. The second change observed in the DSC curves of sGX and sGGM was a sharp endothermic peak at around 170–180 °C, possibly originating from the melting of sGX and sGGM. For celluloses, the DSC curves of MC and CMC powders did not show an indication of glass transition. MC and CMC are crystalline powders, thus they do not have T_g (Olsson & Salmén, 1997). The only noticeable change in the DSC curves of MC and CMC was a sharp melting endothermic peak in the range of 165–175 °C, which is approximately 10 °C less than that of sGX and sGGM. The wall material mixtures (e.g., sGGM + CMC, sGX + CMC, sGGM + MC, and sGX + MC) had a similar T_g to sGX and sGGM (Fig. 1b).

As indicated in Fig. 1a, sGX had a tendency to form semi-crystalline regions upon heating to 170 °C, which was also reported for grafted birch xylans (Persson et al., 2012).

We observed that the tendency of sGX to crystallize in sGX + MC and sGX + CMC was less pronounced than sGX by itself, which could be explained by the smaller amount of sGX in the mixtures. Compared with sGX in both single wall and wall mixtures with celluloses, the tendency to crystallize was less obvious for the sGGM counterparts, which may be due to their differences in amorphous proportions.

The DSC analysis revealed that sGGM and sGX are thermally highly stable. Wall materials with higher T_g enable less stickiness of the produced powders during spray-drying, leading to higher production yields (Hedayatnia et al., 2016). Therefore, in terms of thermal stability, sGGM and sGX are highly applicable for the spray-dried microencapsulation of bioactive compounds in a wide range of inlet and outlet drying temperatures.

Properties of Feed Solutions Prepared Using Various Homogenization Techniques

Total Anthocyanin Content

In this section, we investigated the effects of homogenization techniques and their parameters on anthocyanin stability. Bilberry juice had a TAC of around 1140 mg cyanidin
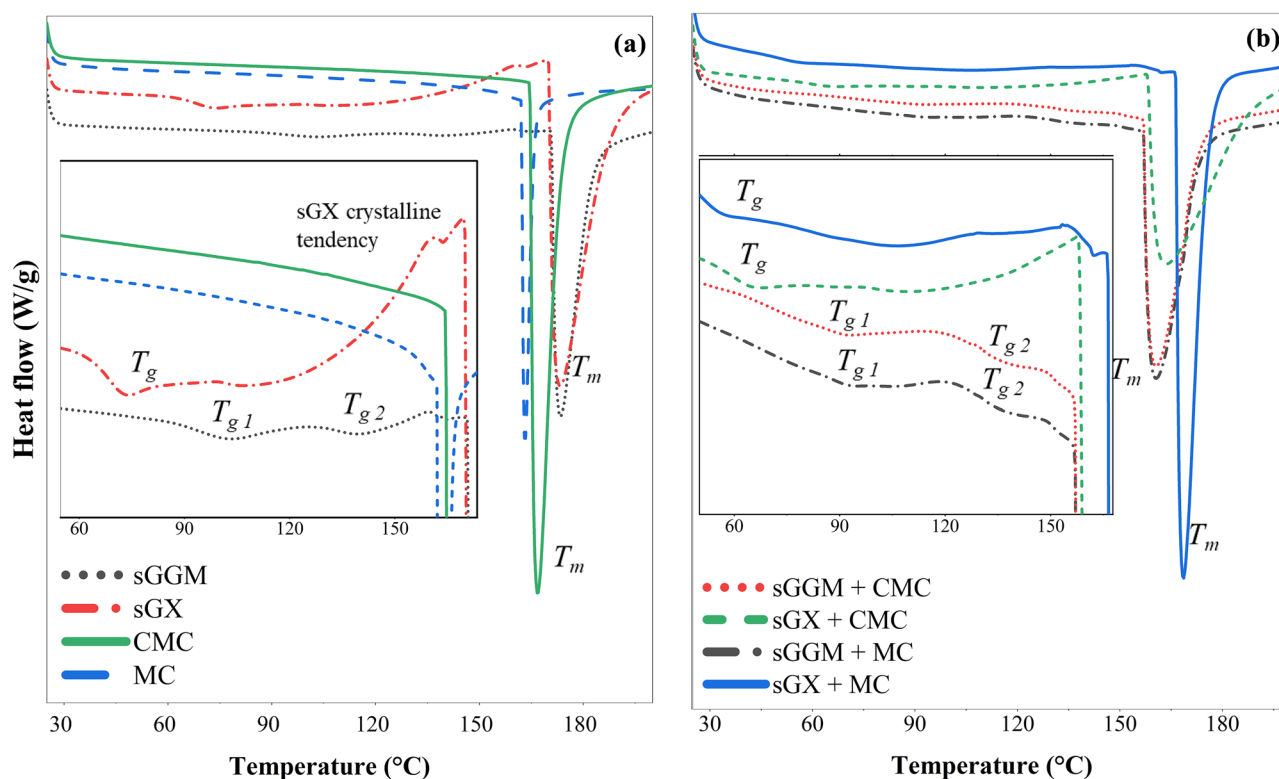

Fig. 1 DSC measurements of **a** single wall materials (sGGM, sGX, MC, and CMC) and **b** wall material mixtures (sGGM+MC, sGGM+CMC, sGX+MC, and sGX+CMC). The small graphs represent the resolution of the original graphs in the range of 60–180 °C, T_g: glass transition temperature, T_m: melting temperature. Refer to Table 1 for sample codes

3-O-glucoside/L. As shown in Fig. 2, magnetic stirring had no effect on TAC; likewise, ultrasonication at different amplitude levels ($p > 0.05$) also had no effects on TAC. Ultrasonication has been used as an alternative or complementary technique in food processing due to its minimal adverse effects on bioactive compounds (Fonteles et al., 2012; Rawson et al., 2011; Tiwari et al., 2009). High-pressure microfluidization showed a large effect on TAC. As the number of microfluidization passes increased from one to five, TAC decreased significantly ($p < 0.05$). For all feed solutions, less than 5%

of TAC was lost with one pass, but a loss of approximately 10–13% and 15–22% of TAC was observed for three and five passes, respectively (Fig. 2). Kruszewski et al. (2021) reported that increasing pressure and the number of microfluidization passes negatively affected the anthocyanins and the color stability of blackcurrant juice. Similarly, Yu et al. (2014) reported that high-pressure homogenization significantly decreased the levels of anthocyanins and phenolic acids in mulberry juice, with a higher degree of reduction observed for a larger number of homogenization passes. The
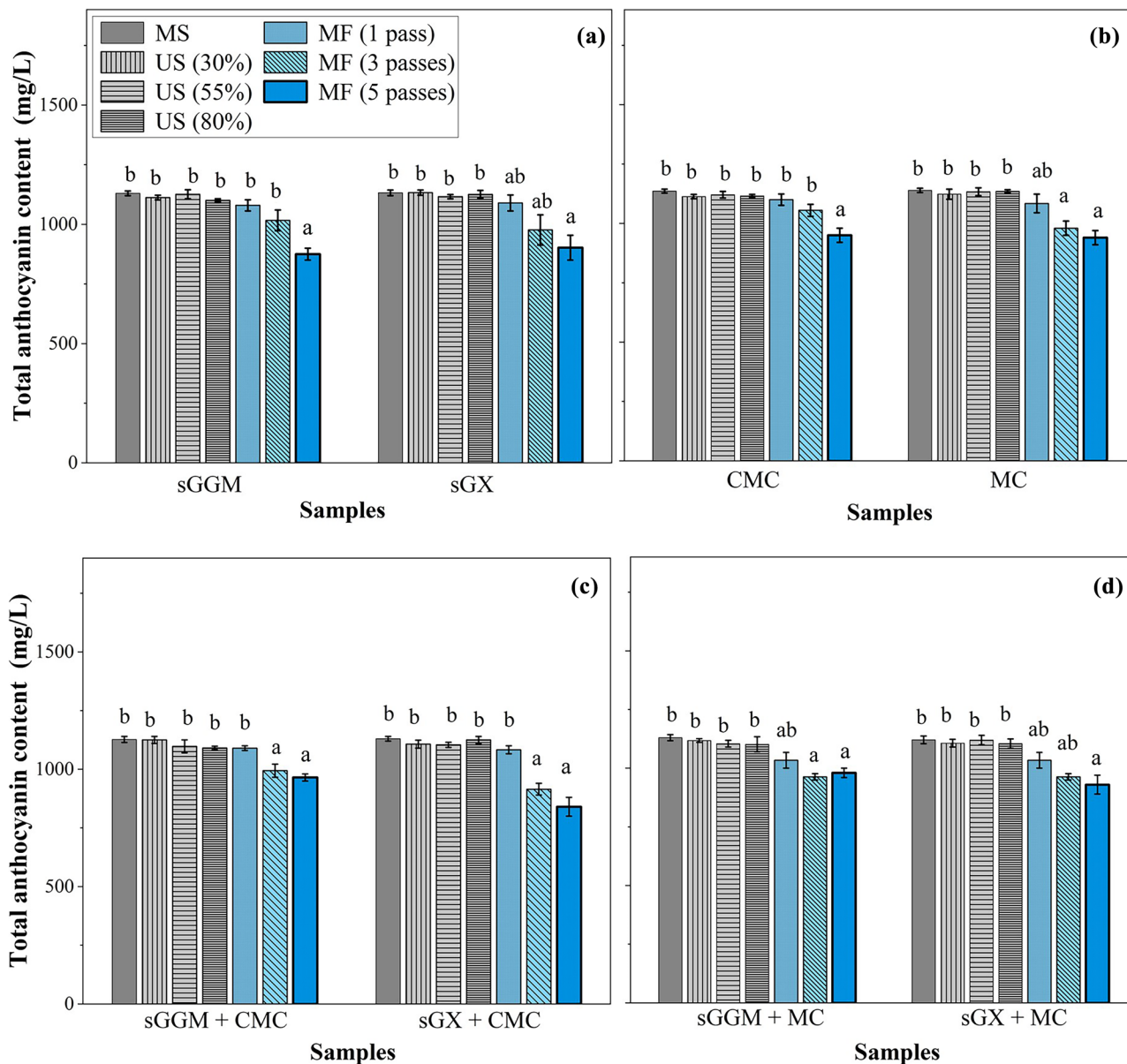

Fig. 2 Total anthocyanin content (TAC) of the feed solutions consisting of **a**, **b** single wall materials (sGGM, sGX, MC, and CMC) and **c**, **d** wall material mixtures (sGGM+MC, sGGM+CMC, sGX+MC, and sGX+CMC) homogenized by magnetic stirring (MS), ultrasonication (US) at three amplitude levels (30%, 55%, and 80%), and microfluidization (MF) at different numbers of passes (1, 3, and 5), number of replicates ($n=3$). Refer to Table 1 for sample codes

loss of anthocyanins in mulberry and strawberry juices under high-pressure homogenization was also reported elsewhere (Terefe et al., 2013; Yu et al., 2014). Anthocyanin degradations are most likely caused by oxidation processes due to oxygen introduced into the juice by the turbulent process of high-pressure homogenization (Kruszewski et al., 2021). In fact, we physically observed foam formation in the feed solutions during mixing by UltraTurrax and homogenizing by microfluidization, indicating that air, including oxygen, was incorporated into the samples. We assume that the effect of mechanical stress on the stability of anthocyanin molecules was negligible, which was also suggested by another study (Yu et al., 2014). In summary, magnetic stirring (600 rpm for 30 min), ultrasonication at different amplitude levels (30%, 55%, and 80%) for 5 min, and one-pass microfluidization at 800 bar had the least effects on anthocyanin stability in feed solutions, and they were therefore selected for investigating other physiochemical properties of feed solutions.

Surface Charge Density

The changes in particle surface charges may be an indicator of electrostatic interactions or adsorption of cationic compounds presenting in bilberry juice onto the wall material surfaces (Sang et al., 2010). The analytical results indicate that the surface charge densities of sGGM and sGX feed solutions were 0.10 and 0.17 meq/g, respectively, suggesting that sGGM and sGX had a small number of charged groups. The sources of charge could be uronic acids and co-extracted phenolic compounds linked naturally to sGGM and sGX, which was also suggested by Bhattarai et al. (2020). Unlike CMC feed solutions, which had high surface charge densities (~ 3.57–4.10 meq/g) owing to the carboxyl groups in the CMC structure, MC feed solutions had very low surface charge (~ 0.02–0.03 meq/g). An aqueous MC solution is uncharged (Kedzior et al., 2017). Therefore, the small surface charge detected in MC feed solutions was mainly due to

the charged compounds present naturally in bilberry juice, such as pectins and other phenolics (Mollov et al., 2006).

As shown in Table 2, the surface charge density values of all the investigated feed solutions prepared by both magnetic stirring and ultrasonication at different amplitude levels were quite similar, but slightly higher than those prepared by microfluidization, especially for sGGM, sGX, and CMC feed solutions. The reduction in surface charge density of the feed solutions prepared by microfluidization in our study may be due to the effects of bilberry juice components under high shearing/turbulent forces of microfluidization. To investigate this hypothesis, we measured the surface charge density of aqueous solutions of sGGM, sGX, and CMC (e.g., without adding bilberry juice) and compared these with their corresponding feed solutions (e.g., by adding bilberry juice). Results showed that the surface charge density of the former was higher than the latter (data not shown). Therefore, microfluidization promotes the electrostatic interactions between the bilberry juice components and wall materials, leading to a decrease in the net surface electrical charge of particles.

ζ-Potential

Higher absolute values of ζ-potential lead to greater electrostatic repulsion between particles, which implies lower agglomeration of particles and higher suspension stability (Vallar et al., 1999). As indicated in Fig. 3, the ζ-potential values of all investigated feed solutions were negative. Regardless of the homogenization methods, CMC feed solutions had the highest absolute ζ-potential, ranging from − 40.5 to − 47.7 mV, while MC feed solutions had the lowest values, ranging from − 4.8 to − 8.4 mV. The absolute ζ-potential of hemicellulose (sGGM and sGX) feed solutions were in the middle range of their MC and CMC counterparts. MC is an uncharged polymer, thus the source of charge in MC feed solutions was primarily from bilberry juice, as the ζ-potential of bilberry juice was found to be from − 6.0

Table 2 Surface charge density (meq/g) of feed solutions prepared with a single wall material and wall material mixtures homogenized by magnetic stirring, ultrasonication at various amplitude levels (30%, 55%, and 80%), and microfluidization

Feed solutions	Magnetic stirring	Microfluidization	Ultrasonication amplitudes (%)		
			30	55	80
sGGM	0.12 ± 0.01^a	0.10 ± 0.01^a	0.15 ± 0.03^a	0.12 ± 0.00^a	0.12 ± 0.01^a
sGX	0.17 ± 0.00^a	0.15 ± 0.04^a	0.17 ± 0.00^a	0.17 ± 0.00^a	0.18 ± 0.00^a
CMC	3.84 ± 0.03^{ab}	3.57 ± 0.06^a	4.10 ± 0.01^c	4.06 ± 0.02^{bc}	3.91 ± 0.11^{bc}
MC	0.03 ± 0.00^a	0.02 ± 0.00^a	0.03 ± 0.00^a	0.02 ± 0.00^a	0.02 ± 0.00^a
sGGM + CMC	1.74 ± 0.03^b	1.47 ± 0.03^a	1.77 ± 0.01^b	1.81 ± 0.02^b	1.79 ± 0.06^b
sGX + CMC	2.35 ± 0.04^a	2.12 ± 0.07^a	2.40 ± 0.05^a	2.39 ± 0.02^a	2.36 ± 0.02^a
sGGM + MC	0.05 ± 0.00^a	0.04 ± 0.00^a	0.06 ± 0.00^a	0.05 ± 0.00^a	0.05 ± 0.00^a
sGX + MC	0.07 ± 0.00^a	0.07 ± 0.00^a	0.06 ± 0.06^a	0.09 ± 0.00^a	0.07 ± 0.00^a

Presented values are the mean and standard error of the mean ($n = 3$). Refer to Table 1 for sample codes. The means with different letters in the same row indicate significant differences at $p < 0.05$
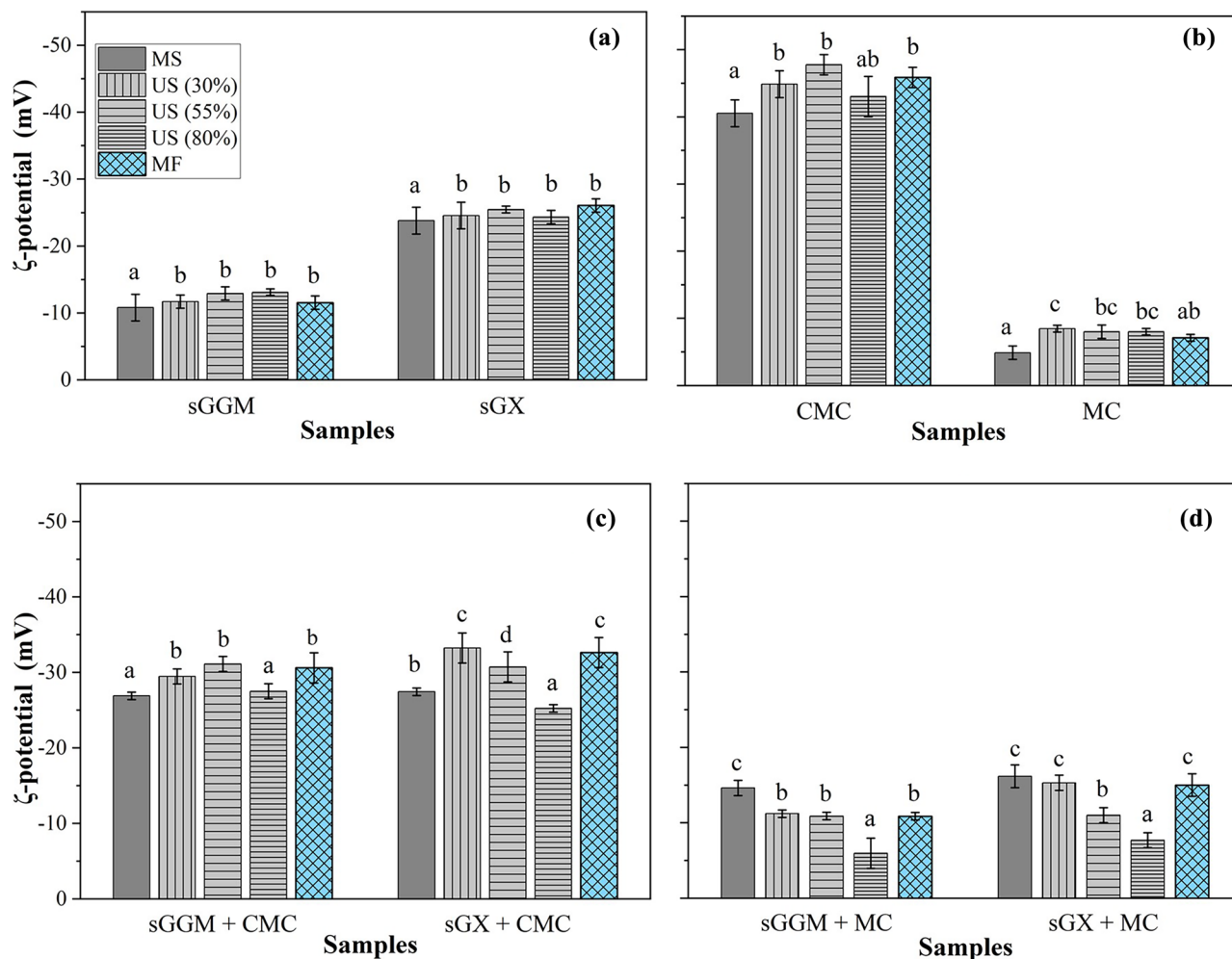
Fig. 3 ζ-Potential of feed solutions of single wall materials (**a**, **b**) (sGGM, sGX, MC, and CMC) and wall material mixtures (**c**, **d**) (sGGM+MC, sGGM+CMC, sGX+MC, and sGX+CMC) homogenized by magnetic stirring (MS), ultrasonication (US) at different amplitude levels (30%, 55%, and 80%), and microfluidization (MF) with one pass. Refer to Table 1 for sample codes

to -8.0 mV. ζ-Potential values of sGGM feed solutions were from -10.9 to -13.1 mV, which is in agreement with values reported by Bhattarai et al. (2020). These values are much lower than those of sGX feed solutions (around -25.0 mV). Dispersion stability can be classified according to its ζ-potential values, by which the dispersions with absolute ζ-potential values of 10, 10–20, 20–30, and 30 mV are categorized as very unstable, fairly stable, moderately stable, and highly stable dispersions, respectively (Bhattacharjee, 2016). According to this classification, the ζ-potential of sGGM feed solutions could not be considered high enough to overcome the attraction forces, and particle agglomeration is expected for sGGM feed solutions over time. Meanwhile, sGX feed solutions were more stable and have less potential for particle agglomeration over time. Regarding homogenization methods, unlike both sGGM and sGX feed solutions, which had similar ζ-potential values among the methods, MC and CMC feed solutions prepared by ultrasonication and

microfluidization had more negative ζ-potential than those prepared by magnetic stirring ($p < 0.05$). This suggests that charged particles, such as CMC, and those naturally present in bilberry juice may have become packed more densely by ultrasonication and microfluidization, which resulted in stretching of the polymer chains and increasing the exposure of functional groups on the particle surfaces.

For wall material mixtures, sGGM+CMC and sGX+CMC feed solutions had similar absolute ζ-potentials, ranging from approximately -26.0 to -33.0 mV (Fig. 3c), which was much higher than the ζ-potentials for sGGM+MC and sGX+MC feed solutions (e.g., -6.9 to -16.1 mV) (Fig. 3d). For homogenization techniques, sGGM+CMC and sGX+CMC feed solutions prepared by magnetic stirring had lower absolute ζ-potentials than the ones prepared by ultrasonication and microfluidization. However, an opposite trend was found for sGGM+MC and sGX+MC feed solutions. These behaviors may result from differences in the preferential adsorption

of MC and CMC on the surface of hemicellulose and/or in their ability to form denser packing on particle surfaces, and therefore they had different contributions to the final surface charge. For effects of ultrasonication, an 80% amplitude led to a decrease in absolute ζ-potential values of feed solutions prepared from wall material mixtures, with a higher extent being observed for sGGM+MC and sGX+MC as compared with the 30% and 55% amplitude levels. Lu et al. (2018) made a similar observation; high ultrasonication powers reduce the magnitude of the negative charge of polysaccharides. This could be explained by increased cellulose adsorption, especially of uncharged ones (e.g., MC), onto the surface of sGGM and sGX at increasing ultrasonication intensity. A similar behavior of MC was observed in a previous study, where the adsorption of uncharged MC onto the surface of charged CNC neutralized the ζ-potential of the CNC solution (Kedzior et al., 2017). Polysaccharides subjected to high-intensity ultrasonication can reportedly undergo a large number of sonochemical reactions including glycosylation, acetalyzation, oxidation, and C–C bond formations (Kardos & Luche, 2001). These reactions affect the charged sites present along the CMC, sGGM, or sGX backbone and/or promote interactions that induce reductions in the number of exposed charged groups for the particles. All these result in magnitudinal changes in ζ-potential (Hosseini et al., 2013).

Both measurements (surface charge density and ζ-potential) were highly correlated in terms of their charge magnitude. As expected, wall materials with higher surface charge density had higher absolute ζ-potential values. However, surface charge density and ζ-potential did not have the same trend among the investigated homogenization techniques. Feed solutions prepared by microfluidization had slightly lower surface charge densities than those prepared by ultrasonication and magnetic stirring. Meanwhile, microfluidization and ultrasonication resulted in higher absolute ζ-potential values than magnetic stirring in all the investigated feed solutions except for sGGM+MC and sGX+MC.

Viscosity

Feed solution viscosity is one of the main properties influencing atomization and drying efficiency (Broniarz-Press et al., 2015; Thompson & Rothstein, 2007). High viscosity of feed solutions could have a negative impact on the droplet formation mechanism, resulting in poor atomization performance and powder properties (Porfirio et al., 2021). The viscosity of all feed solutions is presented in Table 3. Our results indicated that for all homogenization methods, cellulose feed solutions (MC and CMC) had a much higher viscosity than their hemicellulose counterparts (sGGM and sGX). CMC feed solutions had the highest viscosity (e.g., 52.6–79.6 mPa.s), while sGX feed solutions had lowest viscosity (e.g., 1.4–2.0 mPa.s). Unlike sGX feed solutions, whose viscosity was not different among the homogenization conditions, the viscosity of sGGM feed solutions was greatly affected by homogenization techniques, especially ultrasonication amplitudes. For example, the viscosity of sGGM samples prepared at amplitude 80% was 4.4 mPa.s, which was much lower than those prepared at amplitudes 30 and 55% (12.9–17.9 mPa.s). Microfluidization also resulted in considerably higher viscosity of sGGM feed solutions compared with magnetic stirring and ultrasonication at an amplitude of 80%. We assume that the differences in chemical composition and structure of the side chains between sGX and sGGM led to the differences in assembly and aggregation of their molecular chains. The aggregation behaviors of particles are highly correlated with their viscosity. Viscosity was greatly impacted by both the rate and mechanism of particle agglomeration. As the particle agglomeration rate increased, solution viscosity increased (Mills et al., 2000). The supramolecular and microscopic structure of the particles, along with process parameters, such as temperature, strain rate, or frequency during treatments (e.g., microfluidization and ultrasonication), determine particle aggregation (Palzer, 2009).

Table 3 Viscosity (mPa.s) measured at a shear rate of 100 1/s of feed solutions prepared by magnetic stirring, microfluidization, and ultrasonication

Feed solutions	Magnetic stirring	Microfluidization	Ultrasonication amplitudes (%)		
			30	55	80
sGGM	4.1 ± 0.1^a	13.5 ± 2.1^b	17.9 ± 2.1^c	12.9 ± 0.1^b	4.4 ± 0.4^a
sGX	1.4 ± 0.1^a	2.0 ± 0.2^b	1.6 ± 0.2^a	1.5 ± 0.2^a	1.4 ± 0.2^a
MC	40.7 ± 1.3^c	26.3 ± 1.5^{ab}	30.5 ± 1.9^b	28.3 ± 1.5^{ab}	25.6 ± 2.2^a
CMC	79.6 ± 2.1^c	64.9 ± 1.3^b	78.4 ± 2.0^c	73.3 ± 1.6^{bc}	52.6 ± 1.0^a
sGGM+CMC	27.4 ± 2.1^b	25.6 ± 1.8^b	20.4 ± 1.8^b	12.6 ± 0.7^a	11.1 ± 0.6^a
sGX+CMC	24.1 ± 1.6^b	22.2 ± 0.8^b	17.1 ± 10.5^{ab}	12.8 ± 0.9^a	11.3 ± 0.3^a
sGGM+MC	16.7 ± 1.0^{ab}	12.8 ± 1.9^{ab}	21.0 ± 2.5^b	8.4 ± 2.2^a	7.0 ± 0.3^a
sGX+MC	10.1 ± 0.9^a	6.8 ± 0.3^a	8.32 ± 0.3^a	7.9 ± 0.3^a	6.8 ± 0.9^a

Presented values are the mean and standard error of the mean ($n=3$). Refer to Table 1 for sample codes. The means with different letters in the same row indicate significant differences at $p < 0.05$
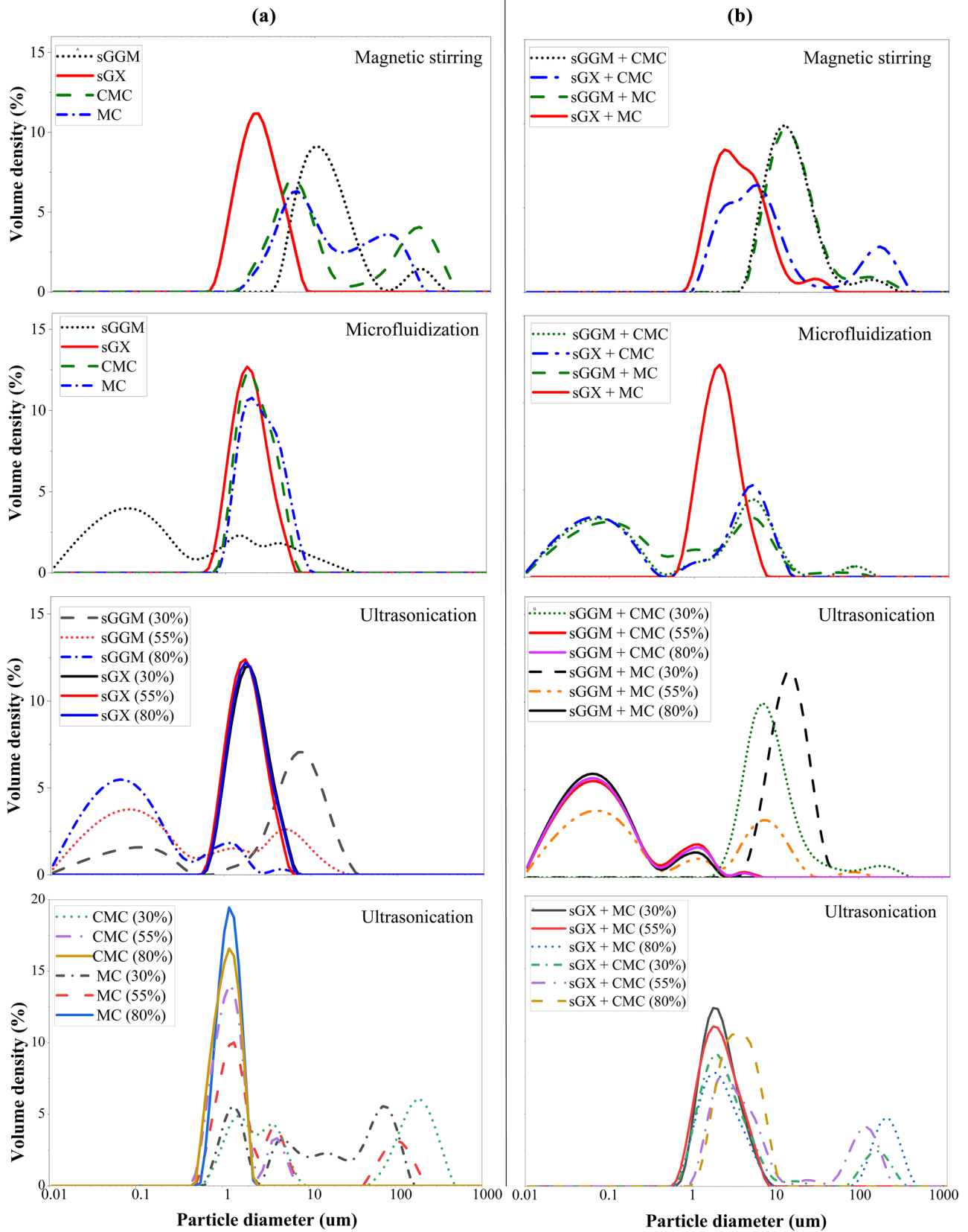
◀**Fig. 4** Particle size distribution of feed solutions consisting of **a** single wall materials (sGGM, sGX, MC, and CMC) and **b** wall material mixtures (sGGM+MC, sGGM+CMC, sGX+MC, and sGX+CMC) homogenized by magnetic stirring, a microfluidization with one pass, and ultrasonication at three amplitude levels (30%, 55%, and 80%). Refer to Table 1 for sample codes

Viscosity of CMC and MC feed solutions followed the same trend under different homogenization techniques. CMC and MC feed solutions obtained either by microfluidization or by increasing the ultrasonication amplitudes had lower viscosity than those subjected to magnetic stirring ($p < 0.05$). The results are in agreement with those reported by Mohod and Gogate (2011) and Mahbubul et al. (2016), reporting that ultrasonication can cause polymer degradation, as reflected by a considerable decrease in intrinsic viscosity and/or molecular weight. Mohod and Gogate (2011) also found that the viscosity of the polymer solution decreased with an increase in ultrasonication time and the shear forces generated during ultrasonication due to rapid motion of the solvent following cavitational collapse, which controls the breakage of the polymer. Likewise, Porfirio et al. (2021) suggested that the reduction in MC viscosity after microfluidization treatment is mainly due to a significant breakdown of the polymer molecules. Similar to MC and CMC feed solutions, microfluidization and ultrasonication lowered the viscosities of sGGM+CMC, sGX+CMC, and sGX+MC feed solutions compared with magnetic stirring.

Among the investigated homogenization techniques, magnetic stirring is the preferred method for homogenizing sGGM feed solutions, as it resulted in the lowest viscosity, which makes spray-drying easier and more efficient. Magnetic stirring remains the preferred method due to its ease, low cost, and because it maintains polymer structure integrity, although the three homogenization techniques had the same effect on sGX feed solutions and ultrasonication and microfluidization lowered the viscosity of CMC and MC feed solutions and their mixtures with sGGM and sGX.

Particle Size Distribution

The particle size distribution curves of all the investigated feed solutions prepared by magnetic stirring, microfluidization, and ultrasonication are presented in Fig. 4. The average values for particle size from the measurements are presented in Table 1S (in the supplementary materials). D[3,2] is the surface area–weighted mean and susceptible to the presence of small particles, while D[4,3] is the volume-weighted mean and sensitive to the presence of large particles (Lahtinen et al., 2019). As indicated in Table 1S, the particle size of sGGM feed solutions homogenized by ultrasonication was highly affected by the ultrasonication amplitudes. For example, the D[3,2] of sGGM feed solutions shifted from 0.21 μm

at an ultrasonication amplitude of 30% to a smaller particle size (0.05 μm) at higher ultrasonication amplitudes (55 and 80%). The D[3,2] and D[4,3] values for sGX feed solutions were similar among the homogenization techniques, which implies that sGX particles were not aggregated and more resistant to structural changes caused by mechanical forces in the homogenization techniques. For particle size distribution of single wall material (Fig. 4a), the sGX feed solution had a monomodal curve with a main peak at approximately 4.0–5.0 μm under all homogenization techniques, including ultrasonication amplitudes. Meanwhile, all sGGM feed solutions had bimodal particle size distribution, but those prepared by magnetic stirring had a main peak at 10 μm, while the main peak of the ones prepared by microfluidization and by increasing the ultrasonication amplitudes shifted to a much smaller particle size range (~0.01–1.0 μm). Li et al. (2017) reported that high ultrasonication power treatment caused a significant reduction in the particle size of konjac glucomannan due to the breakdown of its molecular structure (Li et al., 2017). Similarly, a reduction in particle size with increasing ultrasonication intensity and time was also reported for *Flammulina velutipes* polysaccharides (Chen et al., 2021) and resistant starch (Noor et al., 2021).

The particle size distributions of MC and CMC feed solutions prepared by magnetic stirring and ultrasonication at amplitudes 30 and 55% (Fig. 4a) showed bimodal and/or multimodal (multiple peaks) at large particle sizes (>100 μm), indicating particle agglomeration. Meanwhile, MC and CMC feed solutions prepared by microfluidization and higher ultrasonication amplitude (80%) exhibited one distribution peak at approximately 4.0–6.0 μm. Also, the changes in particle sizes of MC and CMC feed solutions were clearly observed from the Dx (90) values in Table S1. MC and CMC feed solutions prepared by microfluidization had Dx (90) values of 4.29–4.61 μm and 4.15–4.91 μm, respectively, while magnetic stirring and ultrasonication (30 and 55%) resulted in Dx(90) values of 47–96 μm for MC feed solutions and 102–166 μm for CMC feed solutions. As discussed above, high ultrasonication intensity usually reduces the particle size of polysaccharides due to the break in particle aggregates and/or reduction in molecular weight. Also, microfluidization has been demonstrated to be an effective technique in reducing the particle sizes of proteins, lipids, and polysaccharides (Chen et al., 2013; Ciron et al., 2010). We note that particles in the MC and CMC feed solutions are primarily owed to the insoluble particles in bilberry juice. Due to the complete dissolution of MC and CMC in aqueous solution, the particle size of CMC and MC aqueous solution could not be detected by Mastersizer.

Regarding wall material mixtures (Fig. 4b), sGGM+CMC and sGGM+MC feed solutions had similar particle size distributions under each of the investigated homogenization techniques. Microfluidization and ultrasonication (55 and

80%) led to bimodal size distribution in the range of 0.01 to 5 µm, while magnetic stirring and ultrasonication (30%) resulted in a main peak at around 20 µm and a small shoulder at approximately 100 µm. For sGX + CMC and sGX + MC feed solutions, microfluidization caused a shift in particle size distribution to a smaller size range compared with magnetic stirring. For example, the average size values, D[3,2] of sGX + CMC and sGX + MC feed solutions were 0.0675 and 1.66 µm under microfluidization but 4.64 and 2.75 under magnetic stirring. However, the particle size distribution of sGX + CMC was bimodal while that of sGX + MC was monomodal. Regarding the ultrasonication technique, unlike sGGM + CMC and sGGM + MC feed solutions, sGX + CMC and sGX + MC feed solutions show a main peak at around 5–8 µm after ultrasonication at different amplitude levels. However, samples of sGX + CMC feed solutions under ultrasonication (30 and 55%) and sGX + MC under ultrasonication (80%) have shown bimodal size distributions that resulted in a second peak at larger particle sizes (> 100 µm), indicating particle agglomerations, as shown in Fig. 4b. Du Le and Le (2015) reported the agglomeration of mixtures of coconut milk and gelatin solution under various ultrasonication powers (Du Le & Le, 2015). When the ultrasonication power reached "over-processing" levels, the coalescence of droplets enhances the formation of larger droplets or "aggregates" with higher diameter. Ho et al. (2016) reported that ultrasonication pre-treatment improved the self-aggregation of chitosan particles.

Sedimentation Kinetics by Turbiscan

The TSI of feed solutions of single and mixed wall materials prepared by magnetic stirring, microfluidization, and ultrasonication are presented in Fig. 5. The TSI of sGGM feed solutions shows a clear difference between homogenization techniques. For single wall materials (Fig. 5a), although the TSI of sGGM feed solutions homogenized by magnetic stirring was higher compared with microfluidization and ultrasonication, the results cannot be compared because sGGM feed solutions homogenized by ultrasonication and microfluidization formed a gel-like structure over time. An example of sGGM feed solution (10% w/w) gelling after 1 week of ultrasonication treatment is shown in Fig. 6a. Nevertheless, magnetic stirring did not form this kind of strong networking. For sGX feed solutions, the homogenization techniques had nearly the same effect on physical stability and did not induce the formation of a gel-like structure as seen in the sGGM feed solutions. We assume that the effect of cavitation bubbles generated during ultrasonication, and similarly during microfluidization, was one factor contributing to gel formation. Cavitation bubbles are a result of ultrasonic oscillation of the medium to produce periodic compression and stretching (Amiri et al., 2018; Tang, 2007). The periodic production and collapse of cavities generate the shear

forces around the bulk liquid, which were strong enough to break the covalent bonds in the polymeric materials (Amiri et al., 2018). On the other hand, cavitation, alongside shear forces in microfluidization, can cause a certain degree of stretch to polysaccharide molecules, thereby changing the spatial structure of polysaccharide and intermolecular forces (Huang et al., 2018). However, the differences in chemical structure and composition of the side groups between sGGM and sGX are the best explanation available for such sGGM behavior. For example, acetylation levels of sGX are higher than for sGGM, and the molar mass of sGX is lower than sGGM (Du et al., 2013). When dissolved in water, sGX has less insoluble fractions than sGGM. In addition, we have shown throughout our results that sGX had a considerably higher absolute ζ-potential than sGGM, and the homogenization of sGGM feed solutions by ultrasonication and microfluidization resulted in increased viscosities. Furthermore, the particle size distribution of sGGM feed solutions was highly affected by the amplitude levels compared with sGX feed solutions. However, to provide an accurate explanation, further investigation at a molecular level is needed to decipher the gel-formation mechanism of sGGM under mechanical shearing.

CMC and MC feed solutions have shown much lower TSI values compared with sGGM and sGX. This is because CMC and MC are fully dissolved in water, while sGGM and sGX naturally contain insoluble fractions. Cellulose feed solutions also have much higher viscosity than hemicellulose feed solutions, which retards the movement or precipitation of insoluble particles. For cellulosic feed solutions, the MC feed solutions homogenized by magnetic stirring showed two differentiated regions and almost no sedimentation within the first 2 to 3 days, followed by an increase in TSI within the next days of storage. Due to full dissolution of MC molecules, this precipitation is due to the insoluble particles naturally present in bilberry juice. On the other hand, the MC feed solutions homogenized by microfluidization and ultrasonication showed very low TSI values. Meanwhile, all homogenization techniques resulted in the same TSI for the CMC feed solutions. This may be due to CMC being negatively charged (compared with MC), which may electrostatically bind to the juice components. Such an electrostatic network could reduce the precipitation of insoluble juice particles. In addition, the viscosity of CMC at selected concentrations in this study was higher than that of MC, which made it difficult for particle movement or precipitation.

For the wall material mixtures (Fig. 5b), the mixture of sGGM + CMC feed solutions had lower TSI values than the mixture of sGGM + MC for all homogenization techniques, and after 1 week both mixtures still had TSI values below 10 when prepared by ultrasonication and microfluidization compared with magnetic stirring, which had TSI values of 15. The other two mixtures (sGX + CMC and sGX + MC)
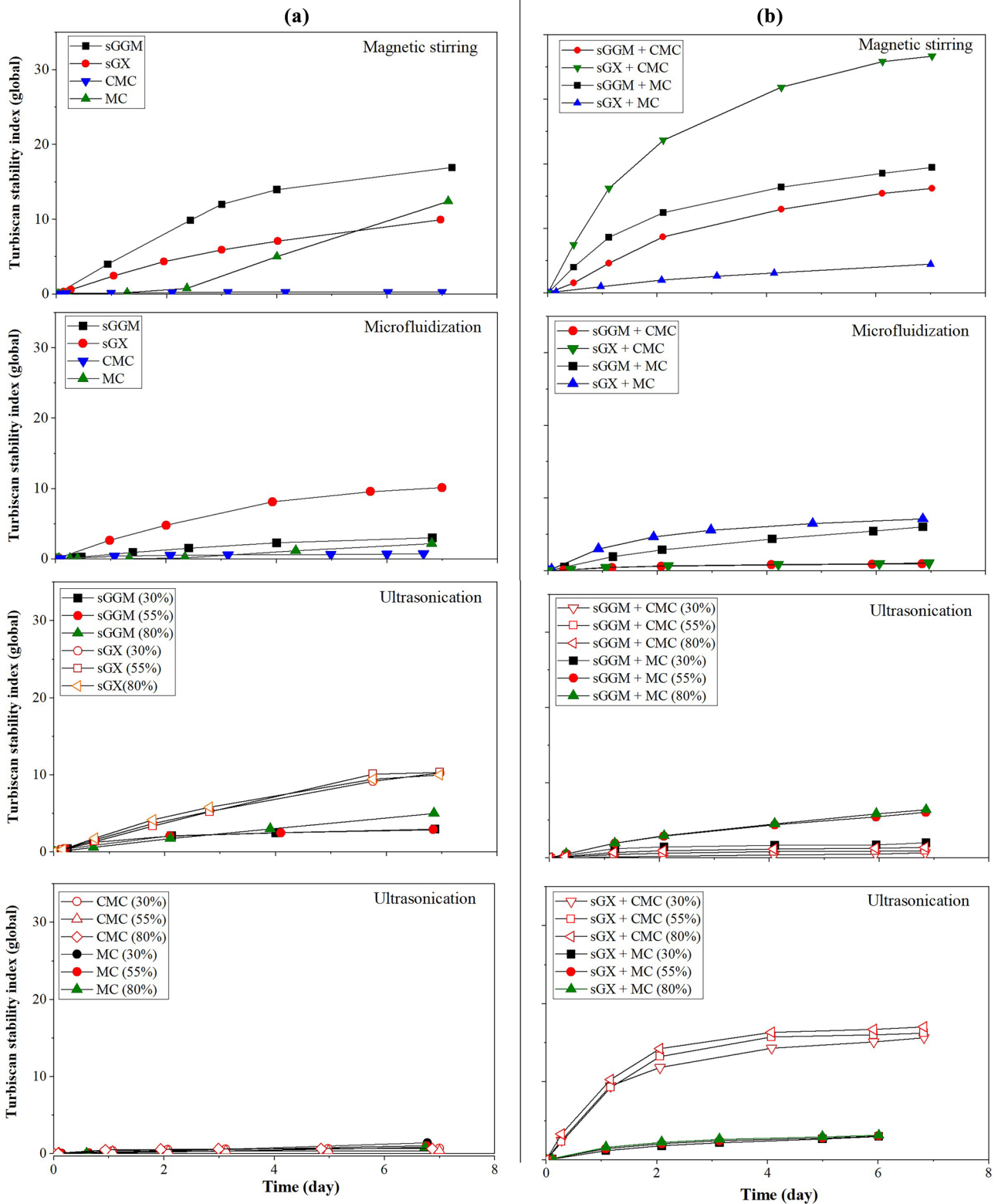
Fig. 5 Turbiscan stability index of the feed solutions consisting of **a** single wall materials (sGGM, sGX, MC, and CMC) and **b** wall material mixtures (sGGM+MC, sGGM+CMC, sGX+MC, and sGX+CMC) homogenized by magnetic stirring, microfluidization with one pass, and ultrasoni-

cation at three amplitude levels (30%, 55%, and 80%) over a 1-week period at room temperature (22 °C). Refer to Table 1 for sample codes
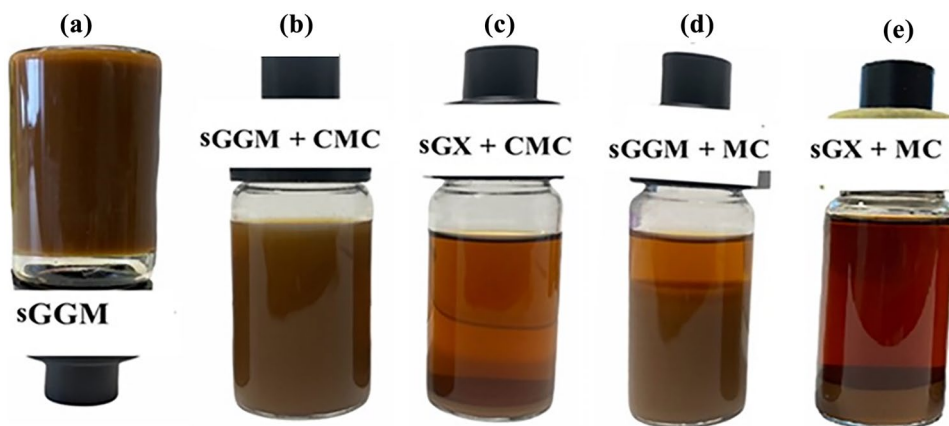
Fig. 6 sGGM (10% w/v) formed a gel-like structure after ultrasonication at an amplitude of 30% for 5 min (**a**), sGGM + CMC aqueous solution (**b**), precipitation of sGX in the mixture of sGX + CMC aqueous solution (**c**), phase separation of sGGM + MC aqueous solution (**d**), and precipitation of sGX in the mixture of sGX + MC aqueous solution (**e**). Aqueous solutions (**b**, **c**, **d**, and **e**) are prepared by magnetic stirring (300 rpm, 30 min), and all photos were taken after 1 week of preparation. Refer to Table 1 for sample codes

display different trends compared with sGGM + CMC and sGGM + MC. For example, sGX + CMC feed solutions obtained by magnetic stirring and ultrasonication had higher TSI values than those of sGX + MC for the same treatment. However, the opposite was found for microfluidization. When we compare the sGX + CMC and sGGM + CMC feed solutions, the former had higher TSI values, especially when prepared by magnetic stirring.

To study the affinity between hemicelluloses (sGGM and sGX) and celluloses (CMC and MC) and the effect of juice, we studied how adding water instead of juice affected the TSI of the feed solution mixtures prepared by magnetic stirring, as this method showed the highest differences in TSI values between the homogenization techniques. Specifically, we studied the sedimentation kinetics of aqueous solutions of sGGM + CMC, sGGM + MC, sGX + CMC, and sGX + MC (without added juice), and the results showed a very high TSI value due to sGX precipitation compared with their feed solutions. This can be examined physically, as indicated in Fig. 6c and e, respectively. As shown in these figures, sGX was highly precipitated when mixed with CMC and MC compared with sGGM, which was much less precipitated when mixed with CMC and MC (Fig. 6b, d). By adding bilberry juice instead of water, the TSI value of the wall material mixtures decreased greatly. The effect of bilberry juice implies that its components were the reason for the stabilization of the wall material mixtures, in addition to the reduction in pH, which changed the nature of the charges compared with water by itself. Moreover, it implies compatibility with the wall materials. Electrostatic interactions are possible between the juice components and wall materials, leading to decreased sedimentation in the solution, and therefore a decrease in TSI. Out of all mixtures, the mixture

of sGGM + CMC feed solution in Fig. 6b homogenized by magnetic stirring showed high affinity between sGGM and CMC. Certain hemicelluloses have previously been demonstrated to have high affinity toward celluloses and to have the ability to alter the properties of cellulose-based products (Naidjonoka et al., 2020). Although the molecular weight of the hemicellulose molecules affects the adsorption behavior, the side groups of the hemicellulose play a crucial role in the degree of affinity (Lucenius et al., 2019).

Feed Solution Stabilities

Three feed solutions including sGGM, sGX, and sGGM + CMC were selected for 1-week stability studies. We selected sGGM + CMC out of the all mixtures because the T_g of sGGM was considerably higher than that of sGX, and the absolute ζ-potential of sGGM + CMC was much higher than that of sGGM + MC. The electrostatic interactions are highly favorable between carboxyl groups and anthocyanins, and thereby the presence of CMC could highly interact with the anthocyanins of juice, leading to an increase in microencapsulation efficiency. Moreover, the solution of sGGM + CMC prepared by magnetic stirring showed high affinity between sGGM and CMC and low TSI value. We therefore predict that the mixture of sGGM + CMC solution is a preferable mixture for spray-dried microencapsulation over the other feed solution mixtures.

During 1 week of storage at room temperature (22 °C), we observed that 10–12% of TAC was lost (Fig. 7a). The ζ-potential and particle size of all the feed solutions were unaffected, as indicated in Fig. 7b and d, respectively. The sGGM feed solution had the highest and sGGM + CMC feed solution the lowest TSI values, while the TSI value of the sGX feed solution was in the middle range of the sGGM
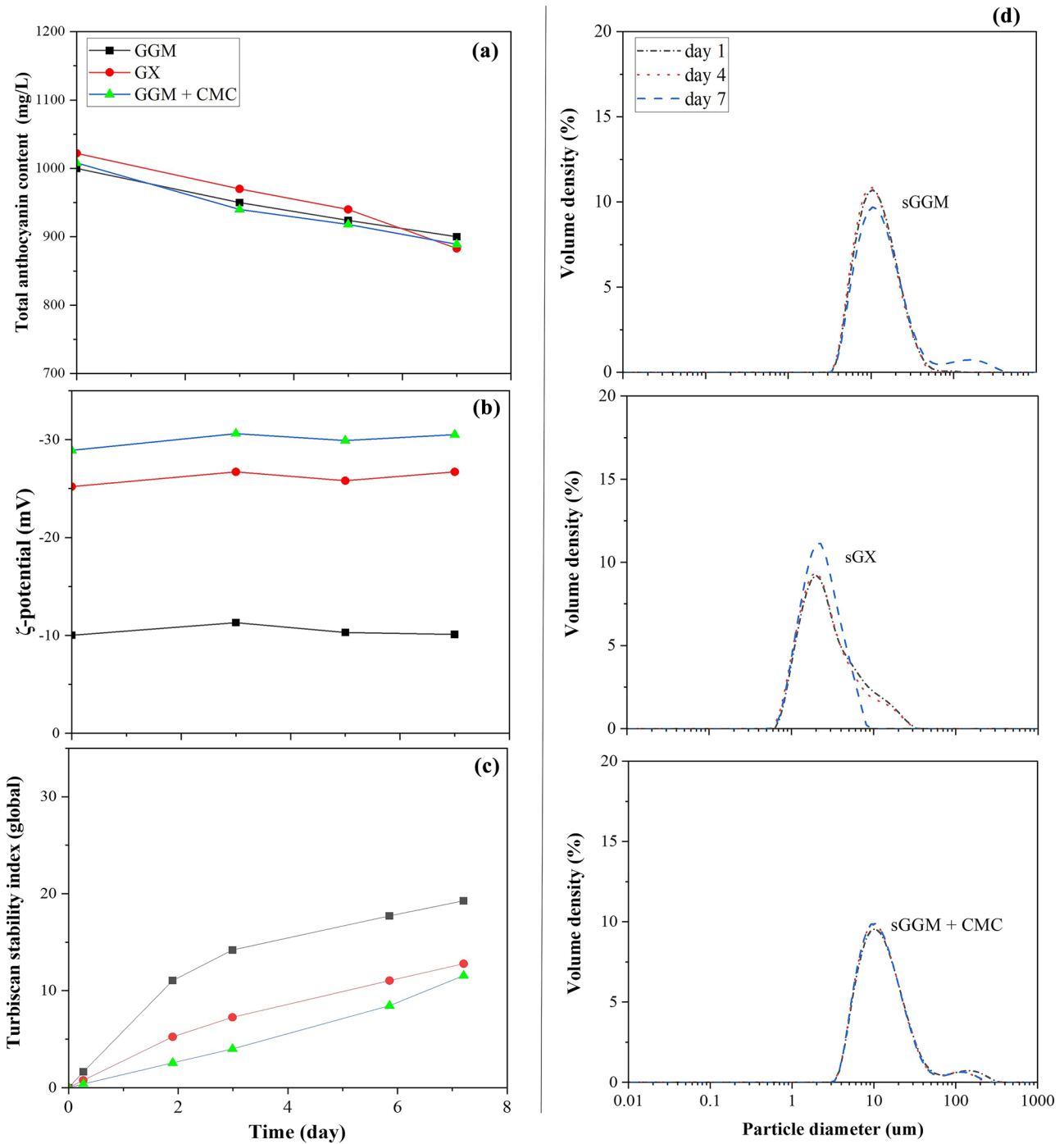
Fig. 7 The stability of feed solutions (sGGM, sGX, sGGM + CMC) prepared by magnetic stirring over 1 week of storage at room temperature: total anthocyanin content (**a**), ζ-potential (**b**), TSI (**c**), and particle size (**d**). Refer to Table 1 for sample codes

and sGGM + CMC feed solutions (Fig. 7c). This is due to sGGM having more insoluble fractions than sGX did. These values are very close to their results in Fig. 5 and are discussed in "Sedimentation Kinetics by Turbiscan" section. The viscosities of sGX and sGGM + CMC were stable over

1 week of storage, except for sGGM feed solutions, which exhibited an increase of viscosity from 4.1 to 9.0 mPa.s during the same period (Table 4). The results indicate that all physicochemical properties of feed solutions were stable, except for anthocyanins.

Table 4 Viscosity (mPa.s) measured at a shear rate of 100 1/s of feed solutions prepared by magnetic stirring measured over 1 week of storage at room temperature

Feed solutions	Storage time (days)			
	Day 1	Day 3	Day 5	Day 7
sGGM	4.1 ± 0.1^a	5.6 ± 0.1^b	7.8 ± 0.1^c	9.0 ± 0.0^d
sGX	1.2 ± 0.0^a	1.3 ± 0.1^a	1.44 ± 0.0^a	1.6 ± 0.0^a
sGGM + CMC	28.9 ± 0.4^a	29.7 ± 0.6^a	30.0 ± 0.5^a	31.9 ± 0.8^b

Presented values are the mean and standard error of the mean ($n = 3$). Refer to Table 1 for sample codes. The means with different letters in the same row indicate significant differences at $p < 0.05$

Conclusions

The valorization of waste products and by-products from lignocellulosic biomass is an essential approach for the acquisition of novel green wall materials. Utilizing these wall materials for spray-dried microencapsulation is more sustainable and cost-effective than using conventional wall materials. In this study, we have demonstrated that wood hemicelluloses including sGGM and sGX have a high potential to be used as wall materials for the spray-dried microencapsulation of core materials rich in bioactive compounds, such as bilberry juice. The research results indicated that magnetic stirring is the best choice for preparing sGGM feed solutions for the spray-dried microencapsulation of bilberry juice. sGGM feed solutions formed a gel-like structure within a short time after ultrasonication and microfluidization, making these solutions unsuitable for spray-drying. Here, we report, for the first time, the formation of gel-like structures from sGGM solution. On the other hand, sGX is highly resistant to changes in the processing parameters, and the three homogenization techniques could be used for preparing sGX feed solutions. Moreover, we have shown that sGGM powders had higher glass transition temperatures than those of sGX. Furthermore, our results also showed that the low viscosity of sGGM and sGX solutions allows for the preparation of feed solutions with high solid ratios of wall materials to bilberry juice. Cellulose (e.g., CMC and MC) solutions have much higher viscosity than sGGM and sGX solutions do, which makes their spray-drying challenging. However, by mixing celluloses with sGGM and sGX, feed solutions with lower viscosity and a high wall material solid ratio could be prepared. We have seen that sGGM, sGX, and sGGM + CMC feed solutions were physically stable over a week of storage, except for anthocyanins, which lost 10–12% of their initial amount, and the viscosity of sGGM feed solution, which was doubled. Further research into spray-dried microencapsulation of bilberry using sGGM, sGX, and a mixture of sGGM + CMC as wall materials is ongoing, to evaluate encapsulation efficiency and the ability to protect the bioactive compounds of these wall materials.

Data Availability The datasets generated during and/or analyzed during the current study are available from the corresponding author on reasonable request.

Declarations

Conflict of Interest The authors declare no competing interests.

References

Agama-Acevedo, E., & Bello-Perez, L. A. (2017). Starch as an emulsions stability: The case of octenyl succinic anhydride (OSA) starch. *Current Opinion in Food Science, 13*, 78–83.

Aghbashlo, M., Mobli, H., Madadlou, A., & Rafiee, S. (2013). Influence of wall material and inlet drying air temperature on the microencapsulation of fish oil by spray drying. *Food and Bioprocess Technology, 6*(6), 1561–1569.

Akhtar, M., Murray, B. S., Afeisume, E. I., & Khew, S. H. (2014). Encapsulation of flavonoid in multiple emulsion using spinning disc reactor technology. *Food Hydrocolloids, 34*, 62–67.

Alcântara, M. A., de Lima, A. E. A., Braga, A. L. M., Tonon, R. V., Galdeano, M. C., da Costa Mattos, M., Santa Brigida, A. I., Rosenhaim, R., dos Santos, N. A., & de Magalhães Cordeiro, A. M. T. (2019). Influence of the emulsion homogenization method on the stability of chia oil microencapsulated by spray drying. *Powder Technology, 354*, 877–885.

Amiri, A., Mousakhani-Ganjeh, A., Torbati, S., Ghaffarinejhad, G., & Kenari, R. E. (2018). Impact of high-intensity ultrasound duration and intensity on the structural properties of whipped cream. *International Dairy Journal, 78*, 152–158.

Aniesrani Delfiya, D., Thangavel, K., Natarajan, N., Kasthuri, R., & Kailappan, R. (2015). Microencapsulation of turmeric oleoresin by spray drying and in vitro release studies of microcapsules. *Journal of Food Process Engineering, 38*(1), 37–48.

Assadpour, E., & Jafari, S. M. (2019). Advances in spray-drying encapsulation of food bioactive ingredients: From microcapsules to nanocapsules. *Annual Review of Food Science and Technology, 10*, 103–131.

Baysan, U., Elmas, F., & Koç, M. (2019). The effect of spray drying conditions on physicochemical properties of encapsulated propolis powder. *Journal of Food Process Engineering, 42*(4), e13024.

Belščak-Cvitanović, A., Lević, S., Kalušević, A., Špoljarić, I., Đorđević, V., Komes, D., & Nedović, V. (2015). Efficiency assessment of natural biopolymers as encapsulants of green tea (Camellia sinensis L.) bioactive compounds by spray drying. *Food and Bioprocess Technology, 8*(12),2444–2460.

Bhattacharjee, S. (2016). DLS and zeta potential–what they are and what they are not? *Journal of Controlled Release, 235*, 337–351.

Bhattarai, M., Pitkänen, L., Kitunen, V., Korpinen, R., Ilvesniemi, H., Kilpeläinen, P. O., Lehtonen, M., & Mikkonen, K. S. (2019). Functionality of spruce galactoglucomannans in oil-in-water emulsions. *Food Hydrocolloids, 86*, 154–161.

Bhattarai, M., Valoppi, F., Hirvonen, S. -P., Hietala, S., Kilpeläinen, P., Aseyev, V., & Mikkonen, K. S. (2020). Time-dependent self-association of spruce galactoglucomannans depends on pH and mechanical shearing. *Food Hydrocolloids, 102*, 105607.

Broniarz-Press, L., Sosnowski, T., Matuszak, M., Ochowiak, M., & Jabłczyńska, K. (2015). The effect of shear and extensional viscosities on atomization of Newtonian and non-Newtonian fluids in ultrasonic inhaler. *International Journal of Pharmaceutics, 485*(1–2), 41–49.

Castro-López, C., Espinoza-González, C., Ramos-González, R., Boone-Villa, V. D., Aguilar-González, M. A., Martínez-Ávila, G. C., & Ventura-Sobrevilla, J. M. (2021). Spray-drying encapsulation of microwave-assisted extracted polyphenols from Moringa oleifera: Influence of tragacanth, locust bean, and carboxymethyl-cellulose formulations. *Food Research International, 144*, 110291.

Chen, J., Gao, D., Yang, L., & Gao, Y. (2013). Effect of microfluidization process on the functional properties of insoluble dietary fiber. *Food Research International, 54*(2), 1821–1827.

Chen, X., Zhao, L., Hu, Q., Xiao, J., Kimatu, B. M., & Zheng, H. (2021). The structure–activity mechanism of the changes in the physicochemical properties of Flammulina velutipes polysaccharides during ultrasonic extraction. *Journal of the Science of Food and Agriculture, 102*(7), 2916–2927.

Ciron, C., Gee, V., Kelly, A., & Auty, M. (2010). Comparison of the effects of high-pressure microfluidization and conventional homogenization of milk on particle size, water retention and texture of non-fat and low-fat yoghurts. *International Dairy Journal, 20*(5), 314–320.

Coimbra, P. P. S., Cardoso, F. d. S. N., & Gonçalves, É. C. B. d. A. (2020). Spray-drying wall materials: relationship with bioactive compounds. *Critical Reviews in Food Science and Nutrition*, 1–18.

Di Battista, C. A., Constenla, D., Ramírez-Rigo, M. V., & Piña, J. (2015). The use of arabic gum, maltodextrin and surfactants in the microencapsulation of phytosterols by spray drying. *Powder Technology, 286*, 193–201.

Du Le, H., & Le, V. V. M. (2015). Application of ultrasound to microencapsulation of coconut milk fat by spray drying method. *Journal of Food Science and Technology, 52*(4), 2474–2478.

Du, X., Gellerstedt, G., & Li, J. (2013). Universal fractionation of lignin–carbohydrate complexes (LCC s) from lignocellulosic biomass: An example using spruce wood. *The Plant Journal, 74*(2), 328–338.

Estevinho, B. N., Rocha, F., Santos, L., & Alves, A. (2013). Microencapsulation with chitosan by spray drying for industry applications–a review. *Trends in Food Science & Technology, 31*(2), 138–155.

Esfanjani, A. F., Assadpour, E., & Jafari, S. M. (2018). Improving the bioavailability of phenolic compounds by loading them within lipid-based nanocarriers. *Trends in Food Science & Technology, 76*, 56–66.

Favaro-Trindade, C. S., Santana, A. D. S., Monterrey-Quintero, E. S., Trindade, M. A., & Netto, F. M. (2010). The use of spray drying technology to reduce bitter taste of casein hydrolysate. *Food Hydrocolloids, 24*(4), 336–340.

Fazaeli, M., Emam-Djomeh, Z., Ashtari, A. K., & Omid, M. (2012). Effect of spray drying conditions and feed composition on the physical properties of black mulberry juice powder. *Food and Bioproducts Processing, 90*(4), 667–675.

Ferrari, C. C., Germer, S. P. M., & de Aguirre, J. M. (2012). Effects of spray-drying conditions on the physicochemical properties of blackberry powder. *Drying Technology, 30*(2), 154–163.

Fonteles, T. V., Costa, M. G. M., de Jesus, A. L. T., de Miranda, M. R. A., Fernandes, F. A. N., & Rodrigues, S. (2012). Power ultrasound processing of cantaloupe melon juice: Effects on quality parameters. *Food Research International, 48*(1), 41–48.

Gabriel, L., Tied, A., & Heinze, T. (2020). Carboxymethylation of polysaccharides–a comparative study. *Cellulose Chemistry and Technology, 54*(9–10), 835–844.

Gambuti, A., Rinaldi, A., Ugliano, M., & Moio, L. (2013). Evolution of phenolic compounds and astringency during aging of red wine: Effect of oxygen exposure before and after bottling. *Journal of Agricultural and Food Chemistry, 61*(8), 1618–1627.

Giusti, M. M., & Wrolstad, R. E. (2001). Characterization and measurement of anthocyanins by UV-visible spectroscopy. *Current protocols in Food Analytical Chemistry*, (1), F1-2.

Gröndahl, M., Teleman, A., & Gatenholm, P. (2003). Effect of acetylation on the material properties of glucuronoxylan from aspen wood. *Carbohydrate Polymers, 52*(4), 359–366.

Halahlah, A., Piironen, V., Mikkonen, K. S., & Ho, T. M. (2022). Polysaccharides as wall materials in spray-dried microencapsulation of bioactive compounds: physicochemical properties and characterization. *Critical Reviews in Food Science and Nutrition*, 1–33.

Hategekimana, J., Masamba, K. G., Ma, J., & Zhong, F. (2015). Encapsulation of vitamin E: Effect of physicochemical properties of wall material on retention and stability. *Carbohydrate Polymers, 124*, 172–179.

Hedayatnia, S., Mirhosseini, H., Tamnak, S., & Golpira, F. (2016). Improvement of glass transition and flowability of reduced-fat coffee creamer: Effect of fat replacer and fluidized bed drying. *Food and Bioprocess Technology, 9*(4), 686–698.

Hindrichsen, I., Wettstein, H., Machmüller, A., Jörg, B., & Kreuzer, M. (2005). Effect of the carbohydrate composition of feed concentratates on methane emission from dairy cows and their slurry. *Environmental Monitoring and Assessment, 107*(1), 329–350.

Ho, K. W., Ooi, C. W., Mwangi, W. W., Leong, W. F., Tey, B. T., & Chan, E. S. (2016). Comparison of self-aggregated chitosan particles prepared with and without ultrasonication pretreatment as Pickering emulsifier. *Food Hydrocolloids, 52*, 827–837.

Hosseini, S. M. H., Emam-Djomeh, Z., Razavi, S. H., Moosavi-Movahedi, A. A., Saboury, A. A., Mohammadifar, M. A., Farahnaky, A., Atri, M. S., & Van der Meeren, P. (2013). Complex coacervation of β-lactoglobulin–κ-carrageenan aqueous mixtures as affected by polysaccharide sonication. *Food Chemistry, 141*(1), 215–222.

Huang, L., Shen, M., Zhang, X., Jiang, L., Song, Q., & Xie, J. (2018). Effect of high-pressure microfluidization treatment on the physicochemical properties and antioxidant activities of polysaccharide from Mesona chinensis Benth. *Carbohydrate Polymers, 200*, 191–199.

Iturri, M. S., Calado, C. M. B., & Prentice, C. (2021). Microparticles of Eugenia stipitata pulp obtained by spray-drying guided by DSC: An analysis of bioactivity and in vitro gastrointestinal digestion. *Food Chemistry, 334*, 127557.

Kardos, N., & Luche, J.-L. (2001). Sonochemistry of carbohydrate compounds. *Carbohydrate Research, 332*(2), 115–131.

Kolanowski, W., Ziolkowski, M., Weißbrodt, J., Kunz, B., & Laufenberg, G. (2006). Microencapsulation of fish oil by spray drying—impact on oxidative stability. Part 1. *European Food Research and Technology, 222*(3), 336–342.

Kedzior, S. A., Dubé, M. A., & Cranston, E. D. (2017). Cellulose nanocrystals and methyl cellulose as costabilizers for nanocomposite latexes with double morphology. *ACS Sustainable Chemistry & Engineering, 5*(11), 10509–10517.

Kilpeläinen, P. O., Hautala, S. S., Byman, O. O., Tanner, L. J., Korpinen, R. I., Lillandt, M. K., Pranovich, A. V., Kitunen, V. H., Willför, S. M., & Ilvesniemi, H. S. (2014). Pressurized hot water flow-through extraction system scale up from the laboratory to the pilot scale. *Green Chemistry, 16*(6), 3186–3194.

Kirjoranta, S., Knaapila, A., Kilpeläinen, P., & Mikkonen, K. S. (2020). Sensory profile of hemicellulose-rich wood extracts in yogurt models. *Cellulose, 27*(13), 7607–7620.

Koç, M., Güngör, Ö., Zungur, A., Yalçın, B., Selek, İ, Ertekin, F. K., & Ötles, S. (2015). Microencapsulation of extra virgin olive oil by spray drying: Effect of wall materials composition, process conditions, and emulsification method. *Food and Bioprocess Technology, 8*(2), 301–318.

Kruszewski, B., Zawada, K., & Karpiński, P. (2021). Impact of high-pressure homogenization parameters on physicochemical characteristics, bioactive compounds content, and antioxidant capacity of blackcurrant juice. *Molecules, 26*(6), 1802.

Lahtinen, M. H., Valoppi, F., Juntti, V., Heikkinen, S., Kilpeläinen, P. O., Maina, N. H., & Mikkonen, K. S. (2019). Lignin-rich PHWE hemicellulose extracts responsible for extended emulsion stabilization. *Frontiers in Chemistry, 7*, 871.

Lee, J., Taip, F., & Abdulla, H. (2018). Effectiveness of additives in spray drying performance: A review. *Food Research, 2*(6), 486–499.

Lehtonen, M., Merinen, M., Kilpeläinen, P. O., Xu, C., Willför, S. M., & Mikkonen, K. S. (2018). Phenolic residues in spruce galactoglucomannans improve stabilization of oil-in-water emulsions. *Journal of Colloid and Interface Science, 512*, 536–547.

Li, J., Li, B., Geng, P., Song, A.-X., & Wu, J.-Y. (2017). Ultrasonic degradation kinetics and rheological profiles of a food polysaccharide (konjac glucomannan) in water. *Food Hydrocolloids, 70*, 14–19.

Lu, H. L., Liu, Z. D., Zhou, Q., & Xu, R. K. (2018). Zeta potential of roots was determined by the streaming potential method in relation to their Mn (II) sorption in 17 crops. *Plant and Soil, 428*(1), 241–251.

Lucenius, J., Valle-Delgado, J. J., Parikka, K., & Österberg, M. (2019). Understanding hemicellulose-cellulose interactions in cellulose nanofibril-based composites. *Journal of Colloid and Interface Science, 555*, 104–114.

Mahdi, A. A., Mohammed, J. K., Al-Ansi, W., Ghaleb, A. D., Al-Maqtari, Q. A., Ma, M., Ahmed, M. I., & Wang, H. (2020). Microencapsulation of fingered citron extract with gum arabic, modified starch, whey protein, and maltodextrin using spray drying. *International Journal of Biological Macromolecules, 152*, 1125–1134.

Mahbubul, I. M., Saidur, R., Amalina, M. A., & Niza, M. E. (2016). Influence of ultrasonication duration on rheological properties of nanofluid: An experimental study with alumina–water nanofluid. *International Communications in Heat and Mass Transfer, 76*, 33–40.

Mikkonen, K. S., Merger, D., Kilpeläinen, P., Murtomäki, L., Schmidt, U. S., & Wilhelm, M. (2016). Determination of physical emulsion stabilization mechanisms of wood hemicelluloses via rheological and interfacial characterization. *Soft Matter, 12*(42), 8690–8700.

Mills, P., Seville, J., Knight, P., & Adams, M. (2000). The effect of binder viscosity on particle agglomeration in a low shear mixer/agglomerator. *Powder Technology, 113*(1–2), 140–147.

Mollov, P., Mihalev, K., Buleva, M., & Petkanchin, I. (2006). Cloud stability of apple juices in relation to their particle charge properties studied by electro-optics. *Food Research International, 39*(5), 519–524.

Mohod, A. V., & Gogate, P. R. (2011). Ultrasonic degradation of polymers: Effect of operating parameters and intensification using additives for carboxymethyl cellulose (CMC) and polyvinyl alcohol (PVA). *Ultrasonics Sonochemistry, 18*(3), 727–734.

Negrão-Murakami, A. N., Nunes, G. L., Pinto, S. S., Murakami, F. S., Amante, E. R., Petrus, J. C. C., Prudêncio, E. S., & Amboni, R. D. (2017). Influence of DE-value of maltodextrin on the physico-chemical properties, antioxidant activity, and storage stability of spray dried concentrated mate (Ilex paraguariensis A. St. Hil.). *LWT-Food Science and Technology, 79*, 561–567.

Naidjonoka, P., Hernandez, M. A., Pálsson, G. K., Heinrich, F., Stålbrand, H., & Nylander, T. (2020). On the interaction of softwood hemicellulose with cellulose surfaces in relation to molecular structure and physicochemical properties of hemicellulose. *Soft Matter, 16*(30), 7063–7076.

Nasatto, P. L., Pignon, F., Silveira, J. L., Duarte, M. E. R., Noseda, M. D., & Rinaudo, M. (2015). Methylcellulose, a cellulose derivative with original physical properties and extended applications. *Polymers, 7*(5), 777–803.

Nogueira, G. F., Soares, C. T., Martin, L. G. P., Fakhouri, F. M., & de Oliveira, R. A. (2020). Influence of spray drying on bioactive compounds of blackberry pulp microencapsulated with arrowroot starch and gum arabic mixture. *Journal of Microencapsulation, 37*(1), 65–76.

Noor, N., Gani, A., Jhan, F., Jenno, J., & Dar, M. A. (2021). Resistant starch type 2 from lotus stem: Ultrasonic effect on physical and nutraceutical properties. *Ultrasonics Sonochemistry, 76*, 105655.

Nunes, G. L., de Araújo Etchepare, M., Cichoski, A. J., Zepka, L. Q., Lopes, E. J., Barin, J. S., de Moraes Flores, É. M., da Silva, C., & d. B., & de Menezes, C. R. (2018). Inulin, hi-maize, and trehalose as thermal protectants for increasing viability of Lactobacillus acidophilus encapsulated by spray drying. *LWT - Food Science and Technology, 89*, 128–133.

Oliveira, C. M., Barros, A. S., Ferreira, A. C. S., & Silva, A. M. (2015). Influence of the temperature and oxygen exposure in red Port wine: A kinetic approach. *Food Research International, 75*, 337–347.

Oliveira, É. R., Fernandes, R. V., Botrel, D. A., Carmo, E. L., Borges, S. V., & Queiroz, F. (2018). Study of different wall matrix biopolymers on the properties of spray-dried pequi oil and on the stability of bioactive compounds. *Food and Bioprocess Technology, 11*(3), 660–679.

Olsson, A.-M., & Salmén, L. (1997). The effect of lignin composition on the viscoelastic properties of wood. *Nordic Pulp & Paper Research Journal, 12*(3), 140–144.

Ovaskainen, M. L., Torronen, R., Koponen, J. M., Sinkko, H., Hellstrom, J., Reinivuo, H., & Mattila, P. (2008). Dietary intake and major food sources of polyphenols in Finnish adults. *The Journal of Nutrition, 138*(3), 562–566.

Palzer, S. (2009). Influence of material properties on the agglomeration of water-soluble amorphous particles. *Powder Technology, 189*(2), 318–326.

Persson, J., Dahlman, O., & Albertsson, A. -C. (2012). Birch xylan grafted with PLA branches of predictable length. *BioResources, 7*(3), 3640–3655.

Porfirio, T., Galindo-Rosales, F. J., Campo-Deaño, L., Vicente, J., & Semião, V. (2021). Rheological characterization of polymeric

solutions used in spray drying process. *European Journal of Pharmaceutical Sciences, 158*, 105650.

Ponder, A., Hallmann, E., Kwolek, M., Średnicka-Tober, D., & Kazimierczak, R. (2021). Genetic differentiation in anthocyanin content among berry fruits. *Current Issues in Molecular Biology, 43*(1), 36–51.

Ramakrishnan, Y., Adzahan, N. M., Yusof, Y. A., & Muhammad, K. (2018). Effect of wall materials on the spray drying efficiency, powder properties and stability of bioactive compounds in tamarillo juice microencapsulation. *Powder Technology, 328*, 406–414.

Rawson, A., Tiwari, B., Patras, A., Brunton, N., Brennan, C., Cullen, P., & O'donnell, C. (2011). Effect of thermosonication on bioactive compounds in watermelon juice. *Food Research International, 44*(5), 1168–1173.

Ribeiro, A. M., Estevinho, B. N., & Rocha, F. (2019). Spray drying encapsulation of elderberry extract and evaluating the release and stability of phenolic compounds in encapsulated powders. *Food and Bioprocess Technology, 12*(8), 1381–1394.

Sang, Y., Qian, L., He, B., & Xiao, H. (2010). The adsorption of cationic PVA on cellulose fibres and its effect with polyelectrolyte complex on paper strength. *Appita: Technology, Innovation, Manufacturing, Environment*, *63*(4).

Sansone, F., Mencherini, T., Picerno, P., d'Amore, M., Aquino, R. P., & Lauro, M. R. (2011). Maltodextrin/pectin microparticles by spray drying as carrier for nutraceutical extracts. *Journal of Food Engineering, 105*(3), 468–476.

Silva, V. M., Vieira, G. S., & Hubinger, M. D. (2014). Influence of different combinations of wall materials and homogenisation pressure on the microencapsulation of green coffee oil by spray drying. *Food Research International, 61*, 132–143.

Song, T., Pranovich, A., Holmbom, B. (2013). Separation of polymeric galactoglucomannans from hot-water extract of spruce wood. *Bioresource Technology, 130*, 198–203.

Stelte, W., Clemons, C., Holm, J. K., Ahrenfeldt, J., Henriksen, U. B., & Sanadi, A. R. (2011). Thermal transitions of the amorphous polymers in wheat straw. *Industrial Crops and Products, 34*(1), 1053–1056.

Strobel, S. A., Hudnall, K., Arbaugh, B., Cunniffe, J. C., Scher, H. B., & Jeoh, T. (2020). Stability of fish oil in calcium alginate microcapsules cross-linked by in situ internal gelation during spray drying. *Food and Bioprocess Technology, 13*(2), 275–287.

Tang, C.-H. (2007). Functional properties and in vitro digestibility of buckwheat protein products: Influence of processing. *Journal of Food Engineering, 82*(4), 568–576.

Teleman, A., Tenkanen, M., Jacobs, A., & Dahlman, O. (2002). Characterization of O-acetyl-(4-O-methylglucurono) xylan isolated from birch and beech. *Carbohydrate Research, 337*(4), 373–377.

Terefe, N. S., Kleintschek, T., Gamage, T., Fanning, K. J., Netzel, G., Versteeg, C., & Netzel, M. (2013). Comparative effects of thermal and high pressure processing on phenolic phytochemicals in different strawberry cultivars. *Innovative Food Science & Emerging Technologies, 19*, 57–65.

Thompson, J. C., & Rothstein, J. P. (2007). The atomization of viscoelastic fluids in flat-fan and hollow-cone spray nozzles. *Journal of Non-Newtonian Fluid Mechanics, 147*(1–2), 11–22.

Tiwari, B., & O'donnell, C., Patras, A., Brunton, N., & Cullen, P. (2009). Stability of anthocyanins and ascorbic acid in sonicated strawberry juice during storage. *European Food Research and Technology, 228*(5), 717–724.

Vallar, S., Houivet, D., El Fallah, J., Kervadec, D., & Haussonne, J.-M. (1999). Oxide slurries stability and powders dispersion: Optimization with zeta potential and rheological measurements. *Journal of the European Ceramic Society, 19*(6–7), 1017–1021.

Valoppi, F., Lahtinen, M. H., Bhattarai, M., Kirjoranta, S. J., Juntti, V. K., Peltonen, L. J., Kilpeläinen, P. O., & Mikkonen, K. S. (2019a). Centrifugal fractionation of softwood extracts improves the biorefinery workflow and yields functional emulsifiers. *Green Chemistry, 21*(17), 4691–4705.

Valoppi, F., Maina, N., Allén, M., Miglioli, R., Kilpeläinen, P. O., & Mikkonen, K. S. (2019b). Spruce galactoglucomannan-stabilized emulsions as essential fatty acid delivery systems for functionalized drinkable yogurt and oat-based beverage. *European Food Research and Technology, 245*(7), 1387–1398.

Waterhouse, G. I., Sun-Waterhouse, D., Su, G., Zhao, H., & Zhao, M. (2017). Spray-drying of antioxidant-rich blueberry waste extracts; interplay between waste pretreatments and spray-drying process. *Food and Bioprocess Technology, 10*(6), 1074–1092.

Xu, C., Eckerman, C., Smeds, A., Reunanen, M., Eklund, P. C., Sjöholm, R., & Willför, S. (2011). Carboxymethylated spruce galactoglucomannans: Preparation, characterisation, dispersion stability, water-in-oil emulsion stability, and sorption on cellulose surface. *Nordic Pulp & Paper Research Journal, 26*(2), 1–12.

Xu, C., Willför, S., Holmlund, P., & Holmbom, B. (2009). Rheological properties of water-soluble spruce O-acetyl galactoglucomannans. *Carbohydrate Polymers, 75*(3), 498–504.

Yu, Y., Xu, Y., Wu, J., Xiao, G., Fu, M., & Zhang, Y. (2014). Effect of ultra-high pressure homogenisation processing on phenolic compounds, antioxidant capacity and anti-glucosidase of mulberry juice. *Food Chemistry, 153*, 114–120.

Zhang, S., Chen, J., Yin, X., Wang, X., Qiu, B., Zhu, L., & Lin, Q. (2017). Microencapsulation of tea tree oil by spray-drying with methyl cellulose as the emulsifier and wall material together with chitosan/alginate. *Journal of Applied Polymer Science*, *134*(13).